

Suspended-load experiments in a curved
flume, run no. 5

A.M. Talmon and J. de Graaff

report no. 1-91, April 1991

part of:

STW-project; River bend morphology with suspended sediment.

Delft University of Technology
Faculty of Civil Engineering
Hydraulic Engineering Division

ABSTRACT

A laboratory experiment in a 180 degree curved flume with a mobile bed and suspended sediment transport is reported. The flow is steady.

The bed topography is measured by means of a profile indicator. Free and forced alternating bars are present. The steady part of the bed topography, which is forced by curvature, is characterized by a below critical response of the transverse bed slope. Downstream of the bend entrance overdeepening occurs, this is weakly repeated further downstream, at these location the transverse bed slope is maximal. Further downstream the transverse bed slope decreases and converges to an approximately constant slope (constant in main flow direction). Suspended sediment concentrations are measured.

<u>CONTENTS</u>	page
ABSTRACT	3
1. INTRODUCTION	10
2. THE LABORATORY EQUIPMENT	
2.1. The flume	11
2.2. Measuring equipment	
2.2.1. Discharge measurement	11
2.2.2. Slope and depth measurements	12
2.2.3. Concentration measurement	12
2.2.4. Temperature measurement	12
2.3. Measuring procedures	13
3. FLOW AND SEDIMENT CONDITIONS	
3.1 A pilot experiment, forced bars in the straight channel	14
3.2 Free and forced bars during bend measurements	14
3.3. The sediment	
3.3.1. Sieve curve	15
3.3.2. Fall velocity	15
3.4. Flow conditions	16
4. RESULTS	
4.1. Depth measurements	
4.1.1. Mean depth	17
4.1.2. Bed form statistics	17
4.2. Concentration measurements	18
5. DISCUSSION	
5.1. Introduction	20
5.2. The Z parameter	20
5.3. Percentage suspended transport	21
5.4. Transport formulae	22
5.5. Bed-shear stress and sediment transport	25

5.6.	Adaptation lengths	27
5.7.	The bed topography	28
6.	CONCLUSIONS	30
	REFERENCES	31
	APPENDIX A Ensemble averaged water depth data	
	APPENDIX B Concentration data	
	APPENDIX C Free bars	
	FIGURES	
	<u>LIST OF TABLES</u>	
3.1a	Measured parameters	16
3.1b	Calculated parameters	16
4.1	Parameter sets of the equilibrium concentration profile	19
5.1	Percentage of suspended sediment transport	22
5.2	The mobility parameter B	26
	<u>LIST OF FIGURES</u>	
1	Layout, Laboratory of Fluid Mechanics curved flume	
2	Sieve curve of sediment	
3	Probability density distribution of fall velocity	
4	Longitudinal water level slope	
5	Contour lines of the relative water depth a/a_0	
6	Longitudinal profile of the water depth	
7a..1	Water depth in cross-direction	
8a	Probability distribution of bed level, cross-section 1...5	
8b	Probability distribution of bed level, flume axis	
9	Concentrations at cross-section 1 and curve fit by Rouse profile	
C1	Bars during pilot experiment	
C2	Bars during bend measurement	

LIST OF SYMBOLS

a	local ensemble mean water depth	[m]
a'	local fluctuation of bed level	[m]
a ₀	mean water depth of cross-section 1 to 5 (in earlier reports: mean depth at cross-section 1)	[m]
\hat{a}	complex amplitude of bed oscillation	[-]
A	critical mobility number	[-]
B	mobility parameter; $B = \tau_{cr}/(\mu r)$	[-]
c	local concentration	[g/l]
c _r	concentration at reference level	[g/l]
\bar{c}	local depth averaged concentration	[g/l]
\bar{c}_{tr}	total transport concentration; $\bar{c}_{tr} = Q_s/Q_w \cdot 10^{-3}$	[g/l]
\bar{c}_{trb}	transport conc. of bed-load; $\bar{c}_{trb} = S_{s \text{ bed}}/(\bar{u}a_0) \cdot 10^{-3}$	[g/l]
\bar{c}_{trs}	transport conc. of suspended-load; $\bar{c}_{trs} = S_{s \text{ sus}}/(\bar{u}a_0) \cdot 10^{-3}$	[g/l]
C	parameter in Ackers White formula	[-]
C	Chézy coefficient, with $d=a_0$; $C = \bar{u}/\sqrt{(di)}$	[m ^{0.5} /s]
d	a representative water depth	[m]
D _{gr}	dimensionless grain diameter; $D_{gr} = D_{50}(\Delta g/\nu^2)^{1/3}$	[-]
D _g	geometric mean grain diameter; $D_g = \sqrt{(D_{84}/D_{16})}$	[m]
D _p	grain size for which p% of the grains is smaller than D _p	[-]
D ₅₀	median grain size	[m]
D _s	sedimentation diameter	[m]
F _g	grain Froude number	[-]
F _{g0}	critical grain Froude number	[-]
F _{gr}	grain mobility number	[-]
Fr	Froude number, with $d=a_0$; $Fr = \bar{u}/\sqrt{(gd)}$	[-]
G	coefficient in gravitation term	[-]
H	depth of the flume	[m]
i	water surface slope	[-]
k	complex wave number	[1/m]
k _b	wave number in transversal direction	[1/m]
k _{sn}	secondary flow convection factor	[-]
L _c	arc length of the bend	[m]
L _{cs}	length scale of adaptation of concentration	[m]
m	parameter in Ackers White formula	[-]
n	parameter in Ackers White formula	[-]
n	coordinate in transverse direction	[m]

P	wetted perimeter	[m]
Q_w	water discharge	[m ³ /s]
Q_s	sediment discharge	[g/s]
r_u	profile function of the velocity profile	[-]
r_c	profile function of the concentration profile	[-]
R_c	radius of curvature of axis of flume	[m]
R_g	grain Reynolds number; $R_g = \sqrt{(gD_{50}^3)/\nu}$	[-]
s	coordinate in streamwise direction	[m]
$S_{s \text{ sus}}$	transport rate of suspended sediment, per unit width, in s-direc.	[g/m/s]
$S_{n \text{ sus}}$	transport rate of suspended sediment, per unit width, in n-direc.	[g/m/s]
S_{tot}	total transport rate, per unit width	[g/m/s]
T	water temperature	[°C]
u	local depth averaged mean flow velocity	[m/s]
\bar{u}	overall averaged mean flow velocity: $\bar{u} = Q_w/(Wa_0)$	[m/s]
u_{cr}	critical depth averaged velocity	[m/s]
u_*	bed friction velocity, based on C : $u_* = (u/g)/C$	[m/s]
W	width of the flume	[m]
w_s	fall velocity of sediment	[m/s]
Z	the Z parameter: $Z = w_s/(\beta\kappa u_*)$	[-]
z_r	reference level	[m]
z_s	surface level	[m]
β	ratio of exchange coefficients of sediment and momentum	[-]
β	coefficient in the bed shear-stress direction model	[-]
κ	von Karman constant	[-]
λ_c	adaptation length of concentration	[m]
λ_s	adaptation length of bed level	[m]
λ_{sf}	adaptation length of bed shear-stress	[m]
λ_w	adaptation length of velocity	[m]
μ	efficiency factor	[-]
ρ	density of water; $\rho = 1000 \text{ kg/m}^3$	[kg/m ³]
ρ_s	density of sediment; $\rho_s = 2650 \text{ kg/m}^3$	[kg/m ³]
σ_g	gradation of sediment; $\sigma_g = D_{84}/D_{16}$	[-]
τ	total drag	[N/m ²]
τ'	effective grain-shear stress; $\tau' = \mu\tau$	[N/m ²]
τ_{cr}	critical bed-shear stress	[N/m ²]

ν_{tm}	turbulent diffusion coefficient of momentum	[m ² /s]
ν_{tc}	turbulent diffusion coefficient of mass	[m ² /s]
θ	Shields number, with $d=a_0$: $\theta = di/(\Delta D_{50})$	[-]
θ_{cr}	critical Shields number	[-]
Δ	relative density of sand; $\Delta = 1.65$	[-]

1. INTRODUCTION

The project at hand is directed towards the computation of river bend morphology in case of alluvial rivers transporting a significant part of their bed material in suspension.

Suspended sediment experiments in previous curved-flume experiments have yielded data on the below critical response of the bed topography. Mild and strongly damping occurred. The latter yields an axi-symmetric region in the 180° flume. An important parameter is the width/depth ratio of the channel. A smaller ratio than in the previous experiments is obtained by using a smaller water depth. According to Olesen's (1987) analysis a less damped response is to be expected. The bed topography and local concentrations of suspended sediment are measured.

In chapter 2 the laboratory equipment is described briefly. In chapter 3 the experimental conditions given. In chapter 4 the results of the measurements of bed topography and concentration are reported. In chapter 5 the results are discussed, attention is being paid to implications regarding the mathematical and numerical simulation of the experiment. In chapter 6 the conclusions are presented.

This research is a part of the project: 'River bend morphology with suspended sediment', project no. DCT59.0842. The project is supported by the Netherlands Technology Foundation (STW).

2. LABORATORY EQUIPMENT

2.1 The flume

The layout of the LFM curved flume is shown in figure 1. Water is pumped from an underground reservoir to an overhead tank and led to the flume. The water discharge is controlled by a valve in the supply pipeline. Sand is supplied to the model 2 m downstream of the entrance of the flume. The sand supply is effectuated by fourteen small holes of 1.6 mm diameter, in the bottom of a container located 0.5 m above the water surface.

After passing the tailgate of the flume, by which the water level is adjusted, the water pours in a settling tank. After passing this tank the water flows back into the underground reservoir.

The dimensions of the flume are:

inflow section length	11.00 m
outflow section length	6.70 m
arc length of the bend	$L_c = 12.88$ m
radius of the bend	$R_c = 4.10$ m
width of the flume	$W = 0.50$ m
depth of the flume	$H = 0.30$ m

The bottom of the flume is made of glass and the side walls are made of perspex.

2.2 Measuring equipment

2.2.1 Discharge measurement

The discharge is controlled by a valve in the supply pipeline. The discharge is measured by a volumetric method. A 150 liters barrel is partly filled during about 30 seconds at the downstream end of the flume. The volume is measured and divided by the filling time.

2.2.2 Slope and depth measurements

The measurements of the bottom and water level are performed with an electronic profile indicator (PROVO). From these measurements the longitudinal slope of the water level and the local depth are calculated. This device is traversed in cross-sectional direction. In each cross-section 9 equidistant measuring points are used. The carriage in which the PROVO is mounted is also traversed in longitudinal direction. In longitudinal direction 48 cross-sections are situated, they are indicated in figure 5. The distance between these cross-sections at the flume axis is 0.32 m. The profile indicator is continuously moved in cross-sectional direction, this is achieved by specially developed electronic hardware. The position of the profile indicator is measured electronically. The carriage is moved manually in longitudinal direction.

2.2.3 Concentration measurements

Sediment concentrations are measured at cross-section 1. Some concentrations are determined by siphoning. Measuring periods of about 45 minutes are employed. The majority is determined by an optical concentration meter OPCON. It has been operated such that prior to each (45 min) measurement a zero concentration adjustment is made. The sensitivity of the OPCON is obtained by calibration. Suspended sediment gathered by the siphoning method is used. The sensitivity of the OPCON is:

$$E = 1.23 c.$$

in which: c [g/l] = concentration

E [V] = voltage at output 10x amplifier

2.2.4 Temperature measurements

Temperatures are measured by inserting a thermometer into the flow near the downstream end of the flume. The water temperature during the measurements was 20.5 ± 0.5 °C .

2.3 Measuring procedure

The flume is partly filled with sand. The thickness of the sand bed at the entrance of the flume is 0.21 m, at the exit the bed thickness is about 0.04 m.

The sand supply is measured daily. The sand settled in the settling tank is gathered at regular intervals (about 32 hours) and is weighed under water. The results are converted to equivalent weights of dry sand. The supply rate is adjusted such that the supply rate and the discharge rate balance.

The water surface slope in longitudinal direction is measured daily. After about 160 hours of flow, measurement of the bed topography and the concentration are started when steady conditions are established. At that stage no significant changes of the water surface slope and differences between in and outflow of sand are measured.

The stationary bed topography is obtained by ensemble averaging of 21 bed level measurements. The time interval between water level measurements is about 7 hours. The interval between bed level measurements is 3...4 hours. To conduct the bed level measurements the flow is stopped, and the flume is filled with water to a higher level than during flow condition. This allows measurement in the shallow parts of the flume.

Each measurement consists of 2 * 48 cross-sectional traverses. Within a cross-section 9 measuring points are used. The data are digitized by an APPLE data-acquisition system. A900 HP mini computer is used to store the data. Further the data are processed by a central main frame IBM computer of the Delft University. From the mean water level in each cross-section the longitudinal slope is determined. Comparing the results of each measuring session, only local differences in the water level slope are noticed.

3. EXPERIMENTAL CONDITIONS

3.1 A pilot experiment, forced bars in the straight reach -----

In order to investigate the wave length and damping of the system the response of the bed topography in the straight channel (10m long) to a steady disturbance is investigated. At the straight channel entrance the flow is obstructed from one side wall to the channel centre-line. This method is identical to that of Struiksma & Crosato (1989) in case of bed load only. The result is a steady alternating bar bed oscillation forced by the disturbance. The wave length of oscillation is 6.5 m. Two periods of oscillation are observed. The second period coincides with point bar and overdeepening locations which are found if no obstruction is present. In the bend beyond cross-section 16 downstream migrating bars start to develop (free bars). Their celerity is about $\approx 0.55 \dots 0.65$ m/h, wave length 3...4 m (appendix C). The amplitude of the forced and free bars is of the order of half the water depth. Wave length and celerity have been determined by visual tracking of the location of the top's and through's of the bars. It is concluded that the selected hydraulic conditions allow for a steady forced oscillation of 6.5 m wave length, its damping cannot be judged because the second period coincides with bars which are forced by the curvature of the flume.

3.2 Free and forced bars during bend measurements -----

The curved flume measurements are conducted without the disturbance in the straight reach. It is tried to eliminate forced bar-formation in the straight reach by preventing sand to accumulate near the sand feeder, when some sand accumulated it was smoothed out by hand. This way it appeared possible to keep the bed flat up to about 4 m downstream of the sand feeder. From this location on, which is still in the straight channel, free bars started to develop and migrate downstream. The bars continued to migrated down to the channel exit. The wave length of the free bars is: 3.2 m, their celerity is 0.64 m/h (appendix C). The steady bars in the bend, which are forced by curvature, are determined by

ensemble averaging of bed-level measurements to filter out free bar contributions.

3.3 The sediment

3.3.1 Sieve curve -----

At the end of the experiment sediment samples were collected from three different sources: the sand supply container, the upper layer of the sediment bed and sediment which is transported in suspension. Figure 2 shows the cumulative probability distributions of the grain sizes of these sediment samples. Characteristic grain diameters are:

	$D_{10}[\mu\text{m}]$	$D_{16}[\mu\text{m}]$	$D_{50}[\mu\text{m}]$	$D_{84}[\mu\text{m}]$	$D_{90}[\mu\text{m}]$	$D_g[\mu\text{m}]$	σ_g
bed layer :	131	143	179	211	223	174	1.48
supply cont. :	124	134	175	209	220	167	1.56
suspended sed.:	117	123	162	197	210	156	1.60

The quantity D_p is defined as the grain size for which p % of the total mixture volume is smaller than D_p .

The geometric mean diameter is defined by: $D_g = \sqrt{(D_{84}D_{16})}$

The gradation of the sediment is defined by: $\sigma_g = D_{84}/D_{16}$

These results indicate that some grain sorting has taken place during the course of the experiments. The sediment of the bed layer has a relatively large number of coarse particles.

3.3.2 Fall velocity -----

The fall velocity of the suspended sediment is determined in a settling tube. This is a device to determine the fall-velocity distribution of particles in a sample. At the lower end of the settling tube the sediment particles accumulate on a very sensitive weighing device. A cumulative weight distribution of the sample as a function of the measuring time is obtained. This distribution is converted into the fall velocity distribution of the sample using the height of the settling tube (Slot and Geldof, 1986).

The sample of suspended sediment is siphoned at about 1 m upstream of cross-section 1. It is siphoned at the centre-line 15 below the water level. The sediment is gathered during 25 hours. The samples are dried and split into amounts that can be used in the settling tube.

Figure 3 shows the probability distribution of the fall velocity of sediment originating from the supply container.

The mean fall velocity, at 20°C, of sediment originating from the supply container is: $w_s = 0.020$ m/s. The mean fall velocity, at 20°C, of suspended sediment is: $w_s = 0.017$ m/s. At higher temperatures the fall velocity increases; 2% per °C. The sedimentation diameter is: $D_s = 176$ μm.

3.4 Flow conditions

The flow conditions are given in table 3.1a and 3.1b. The values of parameters determined by measurement are given in table 3.1a. The values of parameters obtained by calculation are given in table 3.1b.

Table 3.1a Measured parameters

Table 3.1b Calculated parameters

$Q_w = 0.0038$ [m ³ /s]	$\bar{u} = Q_w / (W a_0) = 0.23$ [m/s]
$W = 0.50$ [m]	$\bar{c}_{tr} = (Q_s / Q_w) 10^{-3} = 1.05$ [g/l]
$a_0 = 0.033$ [m]	$C = \bar{u} / \sqrt{(a_0 i)} = 16.3$ [m ^{0.5} /s]
$i = 6.0 \cdot 10^{-3}$ [-]	$Fr = \bar{u} / \sqrt{(g a_0)} = 0.41$ [-]
$D_{50} = 160$ [μm]	$\theta = a_0 i / (\Delta D_{50}) = 0.75$ [-]
$w_s = 17 \cdot 10^{-3}$ [m/s] (20°C susp.)	$u_* = (\bar{u} / g) / C = 0.044$ [m/s]
$Q_s = 4.0$ [g/s]	$D_s = 176$ [μm] (susp., sec. 3.1.2)
$T = 20.5$ [°C]	$Z = w_s / (\beta \kappa u_*) = 0.5$ (sec. 4.2.2)

4. RESULTS

4.1 Depth measurements

4.1.1 Mean depth -----

The ensemble relative water depth of the 21 measuring sessions are tabulated in appendix A. Figure 5 shows the ensemble-averaged contour line map of the relative water depth (normalized with the mean water depth of cross-section 1 to 5). The contour lines are drawn at intervals of $\Delta a/a_0 = 0.2$. The relative depth, at 0.3 W, 0.5 W and 0.7 W, as a function of longitudinal distance is depicted in figure 6. Figures 7a to 7l show the ensemble averaged flow depths of each cross section.

A maximum of the transverse bed slope occurs at cross sections 12 to 14. This is weakly repeated in the region of cross-sections 31 to 33. Further downstream the transverse slope seems to converge to a constant value independent of the longitudinal coordinate. This means that the wave length of oscillation is about 6 m. It corresponds with the 6.5 m wave length of the forced bars observed when the flow is obstructed at the flume entrance.

4.1.2 Bed form statistics -----

The bed consists of free bars and ripples which move downstream. The ripples height is a significant fraction of the flow depth. The shape of these ripples cause a significant form drag to the flow. This is reflected in the low Chézy value; $C = 16.3 \text{ m}^{0.5}/\text{s}$. The large dimensions of the bed forms also affect the choice of reference level, i.e. the level above which the sediment is considered to be transported as suspended load and below which the sediment is considered to be transported as bed-load transport.

To guide the choice of reference level the probability distribution of bed form height is calculated. This is only possible at the channel centre-line because at other locations free bars will also be included. The data of all individual local depth measurements is gathered and

normalized with their local ensemble-averaged value: a'/a . (at each location 21 data points are available, the total number is 1008)

The probability distribution is given in fig.8. Also the distribution in the entrance channel is given, here also data off-centre-line is considered. The distribution at centre-line is indeed somewhat narrower. In fig.8 the 5% and 10% exceedance levels are indicated. These are within the range: $0.4a$ to $0.5a$. It is assumed that these are related to ripples, because diagonal fronts associated with free bars are not observed.

4.2 Concentration measurements

The concentrations are tabulated in appendix B. In fig. 9 the concentrations at cross-section 1 are given. The straight reach prior to the bend entrance serves to establish flow and sediment conditions which are in equilibrium with the local conditions, i.e. the flow and concentration are independent of streamwise coordinates.

To establish the values of parameters of the concentration vertical at equilibrium conditions the measurements in the straight reach are used (cross-section 1). The Rouse concentration profile is fitted with the measurements. This profile is based on the parabolical function for the turbulent exchange coefficient over the vertical.

The parameters of the concentration vertical are:

- the choice of reference height z_r/a
- the concentration at reference height c_r
- the Z parameter, $w_s/(\beta\kappa u_*')$

The concentration profile is given by:

$$c = c_r \left(\frac{z_r}{a_0 - z_r} \frac{a_0 - z}{z} \right)^Z \quad (4.1)$$

Curve fitting has been performed with the aid of a computer program which, given z_r , estimates the Z and c_r parameters of eq.(4.1). A least squares method is employed. Results are given in table 4.1. A curve fit of the concentration data at cross-section 1 is also given in fig. 9, a reference height of $z_r/a_0=0.30$ is applied.

Table 4.1 Parameters of the equilibrium concentration profile

$z_r/a_0 [-]$	$c_r [g/l]$	$Z [-]$	$\bar{c} [g/l]$
0.3	1.4	0.50	0.73

The estimated Z parameter of the concentration vertical is: $Z=0.5$. The reference concentration will vary with the choice of the reference level. The depth-averaged concentration given in table 4.1 is the integral of the concentration curve eq. (4.1) , section 4.2.3. The average value of data points, $z_r/a > 0.3$, is $\bar{c} = 0.69$ g/l. This is nearly equal to the value determined by curve fitting.

5 DISCUSSION

5.1. Introduction

The general purpose of the experiment is to provide data on which numerical and analytical morphological models, including suspended sediment transport, can be calibrated and verified.

Important input parameters of morphological models are:

- The percentage of suspended sediment transport
- The shape of the equilibrium concentration profile
- The transport formula

These subjects are discussed in sections 5.2, 5.3, 5.4 and 5.5.

Adaptation lengths of flow, bed level and concentration are calculated in sec. 5.6. The bed topography is discussed in sec. 5.7. Also a mathematical approximation of the bed topography is given.

5.2. The Z parameter

Curve fitting of the concentration profile prior to bend entrance yields a Z parameter of 0.5 (sec. 4.2.2.). The Z parameter is defined by: $Z = w_s / (\beta \kappa u_*')$. The Z parameter is a measure of the ratio of the downward flux by the fall velocity w_s and the upward flux by turbulent diffusion. Turbulent diffusion of sediment is modelled by:

$$\nu_{tc} = \beta \nu_{tm}, \text{ with } \nu_{tm} = \text{turbulent diffusion of momentum}$$

$$\nu_{tc} = \text{turbulent diffusion of mass (sediment)}$$

It is generally accepted that the turbulent diffusion coefficient of mass is greater than of momentum (Csanady 1973). Consequently $\beta > 1$. In the experiment, upstream of the bend entrance the bed shear velocity is equal to $u_*' = 0.044$ m/s while the fall velocity of the suspended sediment is: $w_s = 0.017$ m/s (from the supply container). This yields $\beta \approx 1.5$

Based on a large data-set van Rijn (1984b) has calculated β by fitting the data with concentration verticals which are based on a parabolical-constant profile for the turbulent diffusion coefficient ν_{tc} . (The present curve fitting is based on a parabolical profile for ν_{tc}). For $w_s/u_* = 0.0172/0.044 = 0.39$ van Rijn reports effective β values in the range of 0.7 ... 1.8 for the experiments of Coleman (1970).

Hinze (1959) reports values of the turbulent Prandtl number $Pr_{turb} = 1/\beta$ of 0.65 to 0.72 ($\beta=1.4$ to 1.5) for various measurements on the distribution of heat and matter in pipe flow and two-dimensional channels.

5.3. Percentage of suspended sediment transport

The percentage of suspended sediment transport upstream of the bend is an important physical parameter of the experiment.

The division between bed and suspended load transport is somewhat arbitrary and is effected by the choice of reference level. The amount of suspended sediment transport per unit width is defined by:

$$S_{s \text{ sus}} = \int_{z_r}^{z_s} u c \, dz \quad (5.1)$$

If curve fitting of the concentration profile is performed the integral of eq.(5.1) can be computed on bases of the integral of the mathematical functions by which the measurements are approximated.

The suspended sediment transport rate per unit width is equal to:

$$S_{s \text{ sus}} = \bar{u} \bar{c} \int_{z_r}^{z_s} r_u r_c \, dz = (a_0 - z_r) \bar{u} \bar{c} \int_0^1 r_u r_c \, d\zeta = (a_0 - z_r) \bar{u} \bar{c} \alpha_s \quad (5.2)$$

with: r_u, r_c shape functions of velocity and concentration

Suspended sediment transport can also be estimated by averaging the measured concentrations in the vertical.

The suspended-sediment transport per unit width is approximated by:

$$S_{s \text{ sus}} \approx \frac{1}{z_s - z_r} \int_{z_r}^{z_s} u \, dz \int_{z_r}^{z_s} c \, dz \approx (z_s - z_r) \bar{u} \bar{c} \quad (5.4)$$

The depth-averaged concentration \bar{c} is computed by the method outlined in subsection 4.2.3.

The objective is to calculate the percentage of suspended-sediment transport. The total transport rate per unit width is equal to:

$$S_{\text{tot}} = a_0 \bar{u} \bar{c}_{\text{tr}} \quad (5.4)$$

in which: \bar{c}_{tr} = the transport concentration defined by eq.(5.4)

The resulting percentage of suspended sediment transport is given in table 5.1.

Table 5.1 Percentage of suspended sediment

method	z_r/a_0	\bar{c} [g/l]	S_s	$S_{\text{sus}}/S_{\text{tot}}$ [%]	remark
curve fitting	0.3	0.73		49 %	Z=0.5, $\alpha_s=1$
summation	0.3	0.69		46 %	

It is concluded that the percentage of suspended sediment transport is about 50 % .

5.4 Transport formulae

To simulate the experiment numerically or analytically a transport formula is necessary to predict concentration and sediment transport rates. In this section the overall transport rate of the experiment is compared with some transport formulae known from literature. It is common practice to express the total sediment transport rate by the transport concentration: $\bar{c}_{\text{tr}} = Q_s/Q_w$ ($S_{\text{tot}} = \bar{c}_{\text{tr}} \bar{u} a_0$ [g/m/s]). The measured transport concentration is equal to: $\bar{c}_{\text{tr}} = 1.05$ g/l.

The transport formulae of Engelund and Hansen (1967), Ackers and White (1973), Brownlie (1981) and Van Rijn (1984c) are evaluated.

These formulae are often employed outside their range of applicability, yielding reasonable results. The Ackers-White and Brownlie formulae are

based on data sets which include data of laboratory flumes with fine sediments.

The Engelund Hansen formula reads:

$$\phi = \frac{0.05}{1-\Gamma} \frac{C^2}{g} \theta^{2.5}, \quad \text{with } \theta = \frac{di}{\Delta D_{50}}, \quad \phi = \frac{S}{\sqrt{(\Delta g D^3)}} \quad (5.6a)$$

$$\text{or: } \bar{c}_{tr} = \rho_s \frac{1}{\bar{u} a_0} 0.05 \sqrt{(\Delta g D_{50}^3)} \frac{C^2}{g} \theta^{2.5} \quad (5.6b)$$

The predicted transport concentration is: $\bar{c}_{tr} = 1.92 \text{ g/l}$
(for D_{50} the value of the supply container is used)

The Ackers White formula reads:

$$\bar{c}_{tr} = \rho_s \frac{D_{50}}{a_0} \left(\frac{\bar{u}}{u_*}\right)^n C \left(\frac{F_{gr}}{A} - 1\right)^m \quad (5.7)$$

$$\begin{aligned} \text{with: } F_{gr} &= \frac{1}{\sqrt{(\Delta g D_{50})}} u_*^n \left(\frac{\bar{u}}{\sqrt{32 \log(10a_0/D_{50})}}\right)^{1-n} = 0.58 \\ A &= 0.23/\sqrt{D_{gr}} + 0.14 = 0.254 \\ n &= 1.00 - 0.56 \log D_{gr} = 0.660 \\ m &= 9.66/D_{gr} + 1.34 = 3.73 \\ C &= 10^{(2.86 \log D_{gr} - \log^2 D_{gr} - 3.52)} = 0.00705 \\ D_{gr} &= D_{50} (\Delta g/\nu^2)^{1/3} = 4.05 \end{aligned}$$

According to White (1972) the formula is fitted to data for which no side wall correction method has been employed, i.e. $d=a_0$. This yields a transport concentration equal to: $\bar{c}_{tr} = 0.53 \text{ g/l}$

The Brownlie formula reads:

$$\bar{c}_{tr} = 7115 (F_g - F_{g0})^{1.978} i^{0.6601} (r_b/D_{50})^{-0.3301} \quad [\text{mg/l}] \quad (5.8)$$

$$\begin{aligned} \text{with: } F_g &= \frac{\bar{u}}{\sqrt{(\Delta g D_{50})}} \quad \text{grain Froude number} \\ F_{g0} &= 4.596 \theta_{cr}^{0.5293} i^{-0.1405} \sigma^{-0.1606} \quad \text{critical grain Froude number} \\ \theta_{cr} &= 0.22 Y + 0.06 (10)^{-7.7 Y} \quad \text{critical Shields number} \\ Y &= (\sqrt{\Delta R_g})^{-0.6} \\ R_g &= \sqrt{(g D_{50}^3)/\nu} \quad \text{grain Reynolds number} \\ r_b &= 0.033 \text{ [m]}, \text{ hydraulic radius related to the bed according to} \\ &\quad \text{Vanoni and Brooks (1957), here } a_0 \text{ is used.} \end{aligned}$$

Prediction with this formula yields: $\bar{c}_{tr} = 0.20 \text{ g/l}$

The Van Rijn (1984c) formulae read:

$$\text{bed-load: } \bar{c}_{trb} = \rho_s 0.005 \left(\frac{u - u_{cr}}{\sqrt{(g\Delta D_{50})}} \right)^{2.4} (D_{50}/a_0)^{1.2} \quad (5.9a)$$

$$\text{suspended-load: } \bar{c}_{trs} = \rho_s 0.012 \left(\frac{u - u_{cr}}{\sqrt{(g\Delta D_{50})}} \right)^{2.4} D_{50}/a_0 d_*^{-0.6} \quad (5.9b)$$

$$\text{total load: } \bar{c}_{tr} = \bar{c}_{trb} + \bar{c}_{trs}$$

$$\text{with: } d_* = D_{50} \sqrt[3]{(\Delta g/\nu^2)}$$

$$u_{cr} = 0.19 D_{50}^{0.1} \log(12r_b/(3D_{90})) = 0.25 \text{ m/s}$$

The transport predicted with these formulae is: $\bar{c}_{tr} = 0$.

This is caused by: $u - u_{cr} < 0$

None of these transport formulae predicts the actual transport concentration of the experiment.

The Brownlie formula underpredicts the transport concentration by a factor 0.2 and Ackers & White by a factor 0.5, while Engelund & Hansen overpredicts by a factor 2.

Prediction of the ratio of suspended-load and total-load can be accomplished by the equations of Van Rijn eq.(5.9a,b). Due, however, to $u_{cr} > u$ this is impossible.

Van Rijn (1984b) has calculated the ratio of suspended-load and total-load of measurements reported by Guy et.al. (1966). It is noticed that for $u_*/w_s > 3$ more than 50% suspended-load is present. This is in accordance with the results of the experiment: $u_*/w_s = 2.6$, $S_{s \text{ sus}}/S_{\text{tot}} \approx 0.50$.

The performance of the transport formulae with regard to this experiment is comparable to the performance of the formulae in case of the other suspended-load experiments.

5.5. Bed-shear stress and sediment transport

In case of a dune covered bed the bed resistance consist of bed shear stress (friction drag) and of a pressure gradient generated by the dunes (shape drag). The total drag (which actually consist of friction and shape drag) is defined by: $\tau = \rho g a i$

The process of sediment transport is caused by the shear stress acting on the grains. The shear stress related to sediment transport is given by: $\tau' = \mu \tau$

in which: μ - efficiency factor

τ' - effective grain-shear stress

τ - total drag.

To initiate sediment transport the shear stress has to exceed a critical value: τ_{cr} .

In the experiment μ is unknown.

One of the reasons of the poor performance of the transport formulae could be caused by the relatively high resistance ($C \approx 16 \text{ m}^{0.5}/\text{s}$). The data on which the transport formulae have been developed generally relate to less ($C \approx 30 \text{ m}^{0.5}/\text{s}$). The transport formulae implicitly, or explicitly, contain the ratio of friction and total drag. This ratio could differ under the present conditions (the relatively large bed form height is quite exceptional). Consequently the effective grain shear-stress will differ also.

In the following sediment transport related parameters μ and θ_{cr} are estimated with the aid of some empirical formulae known from literature.

The transport formulae which incorporate the critical bed-shear stress are generally proportional with:

$$\left(\frac{\mu\tau - \tau_{cr}}{\tau_{cr}}\right)^b = \left(\frac{\mu\theta - \theta_{cr}}{\theta_{cr}}\right)^b = \left(\frac{1-B}{B}\right)^b \quad (5.10a)$$

or:

$$\left(F_g - F_{g0}\right)^b = \left(\frac{u - u_{cr}}{\sqrt{(g\Delta D_{50})}}\right)^b = (1-\sqrt{B})^b \left(\frac{C}{\sqrt{g}} \sqrt{\theta}\right)^b \quad (5.10b)$$

$$\text{in which: } B = \frac{\tau_{cr}}{\mu\tau}, \text{ mobility parameter} \quad (5.10c)$$

Three methods are used to estimate B. The methods are:

- 1)- The set of transport formulae by Van Rijn (1984c), eq.(5.9a,b), is used to relate the total transport concentration c_{tr} and the B parameter. Substitution of the calculated c_{tr} value yields B.
- 2)- The bed-load transport formula by Van Rijn (1984a), eq.(5.10) is used to relate the bed-load transport concentration and the B parameter. Substitution of the calculated c_{trb} value yields B.

$$c_{trb} = \frac{\rho_s}{a u} 0.053 \sqrt{(\Delta g)} \frac{D_{50}^{1.5}}{d_*^{0.3}} \left(\frac{1-B}{B}\right)^{2.1} \quad [g/l] \quad (5.11)$$

- 3)- A relation to estimate the critical Froude grain number by Brownlie (1981) is used.

$$F_{g0} = 4.596 \theta_{cr}^{0.5293} i^{-0.1405} \sigma_g^{-0.1606} \quad (5.12)$$

This relation has been obtained by Brownlie by manipulation of an empirical function which was derived to predict the flow depth.

The results are given in table 5.2. A median grain diameter of $d_{50} = 160 \mu m$ is used. According to the Shields diagram the critical Shields number is: $\theta_{cr} = 0.06$.

Table 5.2 The mobility number B

	method 1	method 2	method 3
B	0.15	0.31	0.19
μ (at $\theta_{cr} = 0.06$)	0.53	0.26	0.42
remark		50 % susp.	
		transp.	

The third method, Brownlie's method, is closely related to Brownlie's water depth prediction. Considering the large error in the depth prediction the estimate of μ is questionable. The results of the first two methods yield different results. The μ parameter is calculated by eq.(5.10c). The μ parameter of the 90 μm experiments, run no. 1 to 3, is

within the range: $0.3 < \mu < 0.4$. For run no. 4 the μ value is within the range: $0.25 < \mu < 0.3$. The van Rijn (1984a) model for μ , which is applied in the Van Rijn transport formulae, yields a distinct result: $\mu = (C/C')^2 = (16/60)^2 = 0.07$. These results indicate that the estimate of μ , implicitly or explicitly contained in the transport formulae, could be erroneous.

The estimated value of μ indicates that about 25...50% of the total drag is available for sediment transport.

5.6 Adaptation lengths

In order to formulate mathematically the interaction of flow and sediment adaptation lengths of flow velocity, bed level and concentration have been defined: Struiksma et.al. (1986) and Olesen (1987). These adaptation lengths are defined as follows:

$$\text{adaptation length of flow: } \lambda_w = \frac{C^2}{2g} a_0 \quad (5.13a)$$

$$\text{adaptation length of bed level: } \lambda_s = \frac{1}{\pi^2} \left(\frac{W}{a_0}\right)^2 \frac{1}{G} a \quad (5.13b)$$

$$\text{adaptation length of concentration: } \lambda_c \approx a \bar{u} / w_s \quad (5.13c)$$

in which: G = coefficient of the gravitational term in the bed-load sediment direction model

The adaptation lengths for flow and bed level in the experiment are:

$$\lambda_w = 0.45 \text{ m}$$

$$\lambda_s = 0.38 \text{ m (for } G=2.0)$$

The adaptation length of concentration depends mainly on the choice of boundary condition for the concentration at reference level (Talmon, 1989). The adaptation length depends further on the value of the Z parameter, the reference height and the Chézy value. The adaptation lengths are calculated based on the assumption of a logarithmic velocity profile and a Rouse distribution for the concentration. To this purpose software which is used in Talmon (1989) has been employed.

Curve fitting of the concentration profile yields: $Z = 0.5$

The Chézy value of the experiment is about: $C = 16.3 \text{ m}^{0.5}/\text{s}$

The reference height should be chosen near the top of the ripples consequently z_r will be in the range: $0.3 < z_r/a < 0.4$, (fig.8)

For $z_r/a=0.35$ and $C=20 \text{ m}^{1/2}/\text{s}$ the adaptation length of the concentration are:

In case of the concentration condition: $\lambda_c = 0.07 \text{ m}$

In case of the gradient condition: $\lambda_c = 0.25 \text{ m}$

5.7 Bed topography

The stationary bed-topography in the 180 degree bend is depicted in fig. 5. A maximum of the transverse bed slope occurs at cross sections 12...14. At this location a point-bar is present in the inner part of the bend. verdeepening occurs at the same location in the outer part of the bend. In cross-section 31...33 again a "weaker" maximum of the transverse slope is noticed. Further downstream the bed slope attains a constant value.

The bed topography is approximated by a damped harmonic wave in longitudinal direction and a linear shape in transverse direction super positioned on an axi-symmetric solution. The latter is also approximated by a linear shape. This yields the following equation:

$$a = (a_0 - \Delta b \frac{n}{\frac{1}{2}W}) e^{iks} + \Delta b_a \frac{n}{\frac{1}{2}W} \quad (5.14)$$

with: Δb = amplitude harmonic solution

Δb_a = amplitude axi-symmetric solution

s = coordinate in streamwise direction ($s=0$ at point bar)

n = coordinate in transverse direction ($n=0$ at centre-line)

k = complex wave number

The last term of eq.(5.14) yields the axi-symmetric bed topography.

Fitting equation (5.14) to the measured bed topography (cross-section 11...46) yields:

$$\text{re}(k) = 1.06 - \frac{2\pi}{5.9}, \quad \text{im}(k) \approx 0.26, \quad \Delta b = 2.5 \text{ cm}, \quad \Delta b_a = 0.65 \text{ cm}$$

The damping $\text{im}(k)$ is difficult to assess, consequently the accuracy is limited. These results indicate a wave length of oscillation of 5.9 m, and 63% damping (e^{-1}) at $s = 4$ m.

6 CONCLUSIONS

The bed topography and sediment concentrations have been measured in a 180 degree curved flume. The median diameter of the sediment is $160 \mu\text{m}$.

The main features of the experiment are:

- The stationary part of the bed topography, which is forced by the curvature, is characterized by a below critical response of the transverse bed slope. Downstream of the bend entrance overdeepening occurs, this is weakly repeated further downstream, at these locations the transverse bed slope is maximal. Further downstream the transverse bed slope decreases and converges to an approximately constant slope (constant in main flow direction).
- Non-stationary bars (free bars) are present.
- Wave length of forced and free bars and the celerity of free bars correspond to bars observed in a pilot experiment in which the flow in the entrance of the straight channel was partly blocked.

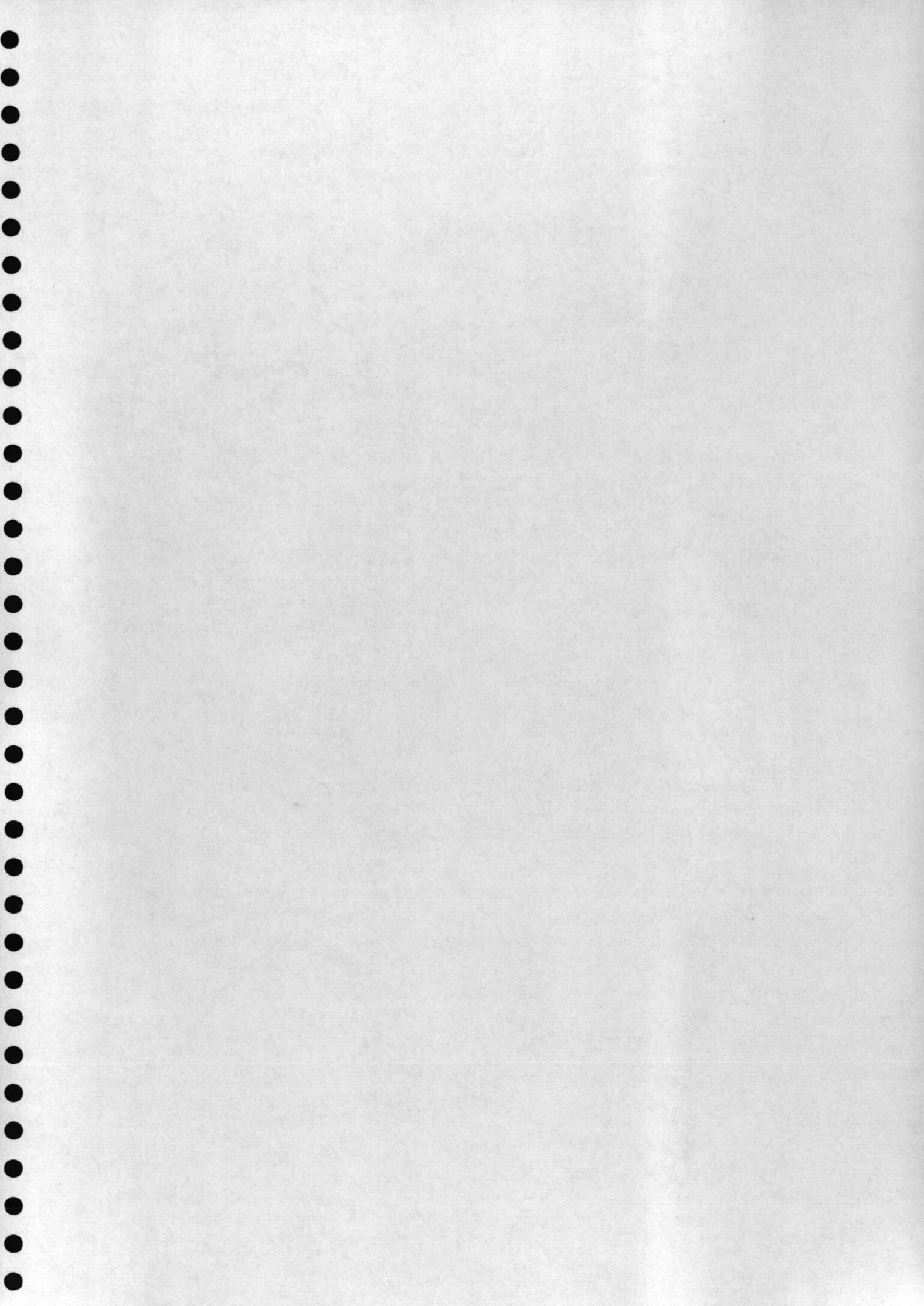
The following parameter values characterize the experiment.

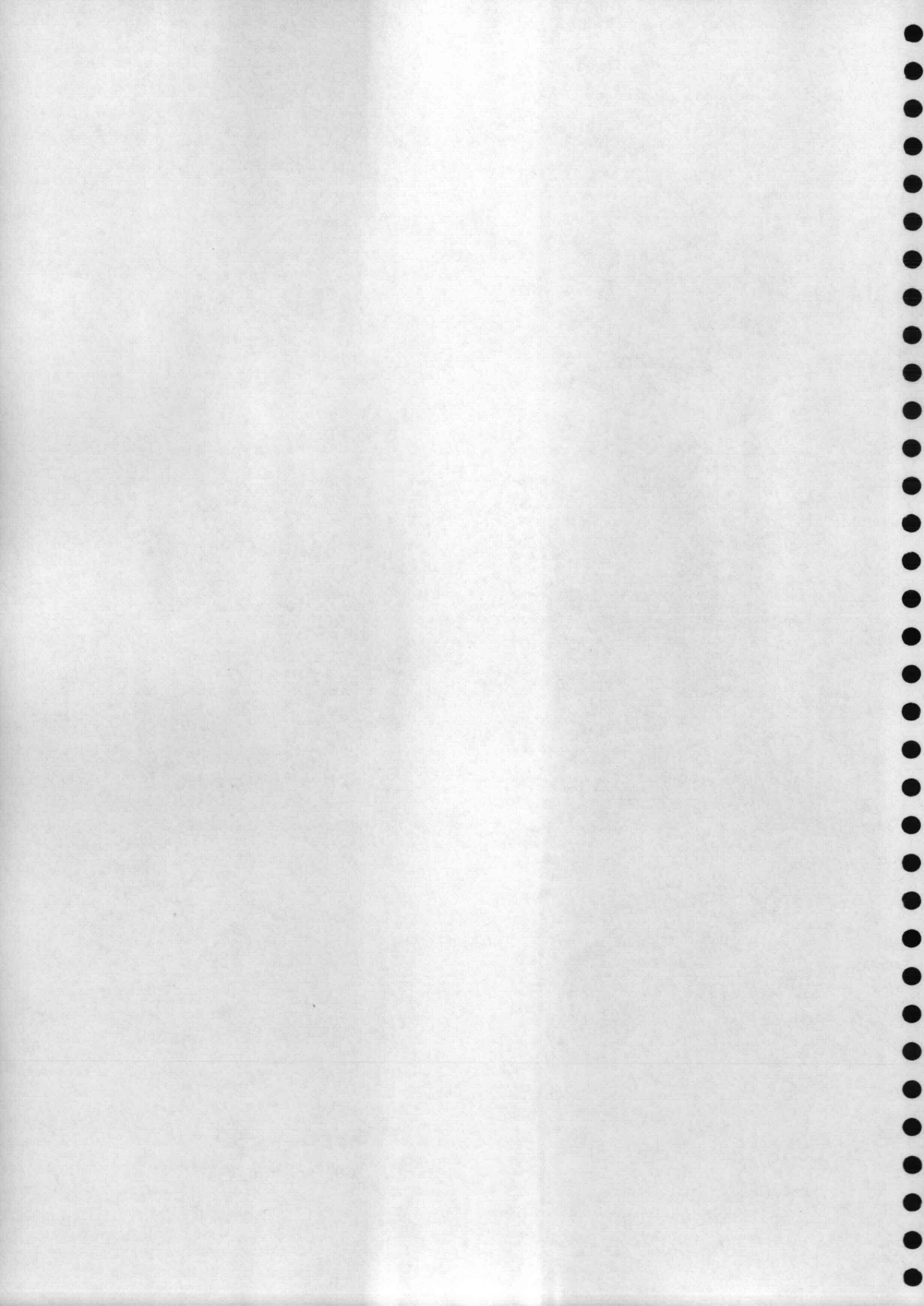
- The Chézy value is about: $C = 16.3 \text{ m}^{0.5}/\text{s}$
- With the aid of curve fitting the Z parameter of the equilibrium concentration-profile is estimated to be: $Z = 0.5$
- Due to the exaggerated bed-form dimensions the reference height should be chosen within: $0.3 < z_r/a < 0.4$
- The percentage suspended-sediment transport is about 50 % .

REFERENCES

- Ackers, P. and W.R. White, 1973, Sediment transport: a new approach and analysis, *Journal of the Hydraulics Division, ASCE*, vol. 99, no. HY11, pp. 2041-2060.
- Brownlie, W.R., 1981, Prediction of flow depth and sediment discharge in open channels, W.M. Keck Laboratory of Hydraulics and Water Resources, California Institute Of Technology, Pasadena California, rep. no. KH-R-43A.
- Coleman, N.L., 1970, Flume studies of the sediment transfer coefficient *Water Resources*, Vol 6, no 3.
- Csanady, G.T., 1973, *Turbulent diffusion in the environment*, D. Reidel Publishing Co., Dordrecht, the Netherlands.
- Delft Hydraulics, 1986, Optical concentration meter, model OPCON, Technical manual.
- Engelund, F. and E. Hansen, 1967, A monograph on sediment transport in alluvial streams, Teknisk Forlag, Copenhagen, Denmark, pp. 62.
- Guy, H.P., D.B. Simons and E.V. Richardson, 1966, Summary of alluvial channel data from flume experiments, 1956-1961, *Geological Survey Professional Paper 462-I*, Washington, D.C. pp. 93.
- Olesen, K.W., Bed topography in shallow river bends
Doctoral thesis Delft University of Technology, 1987
(also: ISSN 0169-6548 *Communications on Hydraulic and Geotechnical Engineering*, Delft University of Technology, Faculty of Civil Engineering).
- Rijn, L.C. van, 1984a, Sediment transport, part I: bed load transport, *Journal of Hydraulic Engineering*, Vol 110, no. 10, pp. 1431-1456.
- Rijn, L.C. van, 1984b, Sediment transport, part II: suspended load transport, *Journal of Hydraulic Engineering*, Vol 110, no. 11, pp. 1613-1641.
- Rijn, L.C. van, 1984c, Sediment transport, part III: bed form and alluvial roughness, *Journal of Hydraulic Engineering*, Vol 110, no. 12, pp. 1733-1754.
- Rijn, L.C. van, 1987, Mathematical modelling of morphological processes in the case of suspended sediment transport
Doctoral thesis Delft University of Technology, 1987
(also: Delft Hydraulics Communication no. 382).

- Slot, R.E. and H.J.Geldof, 1986, An improved settling tube system for sand. ISSN 0169-6548, Communications on Hydraulics and Geotechnical Engineering, Delft University of Technology, Faculty of Civil Engineering, rep. no. 86-12.
- Struiksma, N. and A. Crosato, 1989, Analysis of a 2-DH bed topography model for rivers, in: River Meandering, A.G.U. Water resources monograph, vol. 12, Washington D.C., U.S.A.
- Struiksma, N.; K.W. Olesen, C. Flokstra and H.J. de Vriend, 1986, Bed deformation in alluvial channel bends. IAHR, Journal of Hydraulic Research, vol. 23, no. 1, pp. 57-79.
- Talmon, A.M., 1989, A theoretical model for suspended sediment transport in river bends, ISSN 0169-6548, Communications on Hydraulic and Geotechnical Engineering, Delft University of Technology, Faculty of Civil Engineering, rep. no. 89-5.
- Vanoni, V.A. and N.H. Brooks, 1957, Laboratory studies of the roughness and suspended load of alluvial streams, Rep. no. E-68, Publication no. 149, California Institute of Technology Pasadena, California, pp. 121.
- White, W.R., 1972, Sediment transport in channels: a general function, rep. INT 104, Hydraulics Research Station, England.





Appendix A: Ensemble-averaged water depths.

In this appendix the ensemble-averaged relative water depths of the 21 measurements are tabulated.

Relative mean water depth a/a_0 . ($a_0 = 0.033$ m)

from inner side of bend	CS01	CS02	CS03	CS04	CS05	CS06	CS07
0.05	1.21	1.10	1.17	1.16	1.26	1.15	1.13
0.10	1.18	1.10	1.19	1.16	1.19	1.17	1.11
0.15	1.04	1.09	1.13	1.07	1.02	1.16	1.08
0.20	1.03	0.97	0.94	0.92	1.00	1.04	0.97
0.25	1.06	0.94	0.94	0.90	0.97	0.91	0.85
0.30	0.99	0.93	1.00	0.89	0.93	0.90	0.78
0.35	0.89	0.95	0.87	0.96	0.84	0.85	0.83
0.40	0.87	0.92	0.90	0.94	0.87	0.81	0.92
0.45	0.92	0.92	0.91	0.90	0.87	0.82	0.96

from inner side of bend	CS08	CS09	CS10	CS11	CS12	CS13	CS14
0.05	1.03	0.88	0.73	0.60	0.53	0.56	0.61
0.10	1.00	0.89	0.80	0.62	0.64	0.53	0.57
0.15	1.11	0.94	0.91	0.75	0.68	0.58	0.58
0.20	1.05	0.92	0.82	0.81	0.69	0.73	0.68
0.25	0.90	0.98	0.86	0.94	0.83	0.81	0.92
0.30	0.88	0.93	0.98	1.01	0.97	0.91	1.05
0.35	0.95	1.00	1.16	1.13	1.21	1.24	1.28
0.40	1.02	1.05	1.25	1.32	1.47	1.42	1.36
0.45	1.17	1.26	1.45	1.60	1.59	1.62	1.56

from inner side of bend	CS15	CS16	CS17	CS18	CS19	CS20	CS21
0.05	0.76	0.93	1.00	0.90	0.89	0.98	1.05
0.10	0.73	0.81	0.96	0.94	0.88	0.92	0.94
0.15	0.68	0.77	0.87	1.03	0.92	0.92	0.87
0.20	0.79	0.77	0.84	0.91	0.84	0.90	0.90
0.25	0.90	0.86	0.83	0.87	0.86	0.90	0.99
0.30	0.96	1.05	0.84	0.92	0.96	1.00	0.97
0.35	1.14	1.19	1.01	1.07	1.11	1.00	1.11
0.40	1.31	1.30	1.05	1.08	1.16	1.13	1.05
0.45	1.47	1.31	1.15	1.20	1.17	1.21	1.10

from inner side of bend	CS22	CS23	CS24	CS25	CS26	CS27	CS28
0.05	1.02	0.98	1.07	0.86	0.96	0.86	0.94
0.10	0.98	0.94	0.98	0.90	0.97	0.90	0.83
0.15	1.00	0.97	1.01	0.95	0.91	0.96	0.89
0.20	0.80	0.99	0.99	1.02	0.96	1.03	0.96
0.25	0.96	1.00	0.98	0.96	1.03	0.97	1.00
0.30	1.01	1.00	0.92	0.95	1.03	0.92	1.03
0.35	0.99	1.00	1.00	1.04	1.06	1.00	1.16
0.40	1.03	1.04	1.07	1.10	1.09	1.20	1.10
0.45	1.13	1.09	1.02	1.10	1.09	1.16	1.16

from inner side of bend	CS29	CS30	CS31	CS32	CS33	CS34	CS35
0.05	0.74	0.68	0.73	0.72	0.82	0.95	0.89
0.10	0.80	0.74	0.76	0.69	0.78	0.86	0.83
0.15	0.91	0.81	0.78	0.76	0.78	0.86	0.86
0.20	0.88	0.98	0.90	0.81	0.85	0.78	0.89
0.25	0.91	0.92	0.97	1.05	1.03	0.91	0.89
0.30	1.00	1.05	1.04	1.08	1.04	1.05	0.94
0.35	1.00	1.01	1.11	1.17	1.17	1.19	1.06
0.40	1.24	1.11	1.17	1.26	1.28	1.24	1.18
0.45	1.23	1.23	1.31	1.42	1.37	1.36	1.20

from inner side of bend	CS36	CS37	CS38	CS39	CS40	CS41	CS42
0.05	0.89	0.88	0.90	0.76	0.89	0.98	0.89
0.10	0.88	0.90	0.93	0.77	0.92	0.90	0.85
0.15	0.86	0.90	0.89	0.84	0.90	0.92	0.88
0.20	0.92	1.01	0.98	0.94	0.92	0.99	1.01
0.25	0.93	0.99	0.99	0.95	1.03	0.95	1.12
0.30	0.97	1.02	0.99	1.04	1.00	0.97	1.09
0.35	1.09	1.03	1.07	1.05	1.24	1.19	1.11
0.40	1.12	1.15	1.06	1.25	1.23	1.16	1.16
0.45	1.23	1.25	1.13	1.30	1.26	1.21	1.21

from inner side of bend	CS43	CS44	CS45	CS46	CS47	CS48
0.05	0.82	0.82	0.84	0.85	1.04	1.07
0.10	0.87	0.89	0.86	0.82	0.84	0.96
0.15	0.89	0.88	0.94	0.95	0.83	0.98
0.20	0.87	0.89	0.93	1.01	0.94	0.96
0.25	0.91	1.00	0.97	1.02	0.98	0.98
0.30	0.97	1.16	1.04	1.12	1.09	1.04
0.35	1.08	1.18	1.11	1.15	1.12	1.14
0.40	1.21	1.19	1.21	1.13	1.09	1.04
0.45	1.16	1.29	1.24	1.10	1.14	1.06

Appendix B: Concentration dataCross section 1.

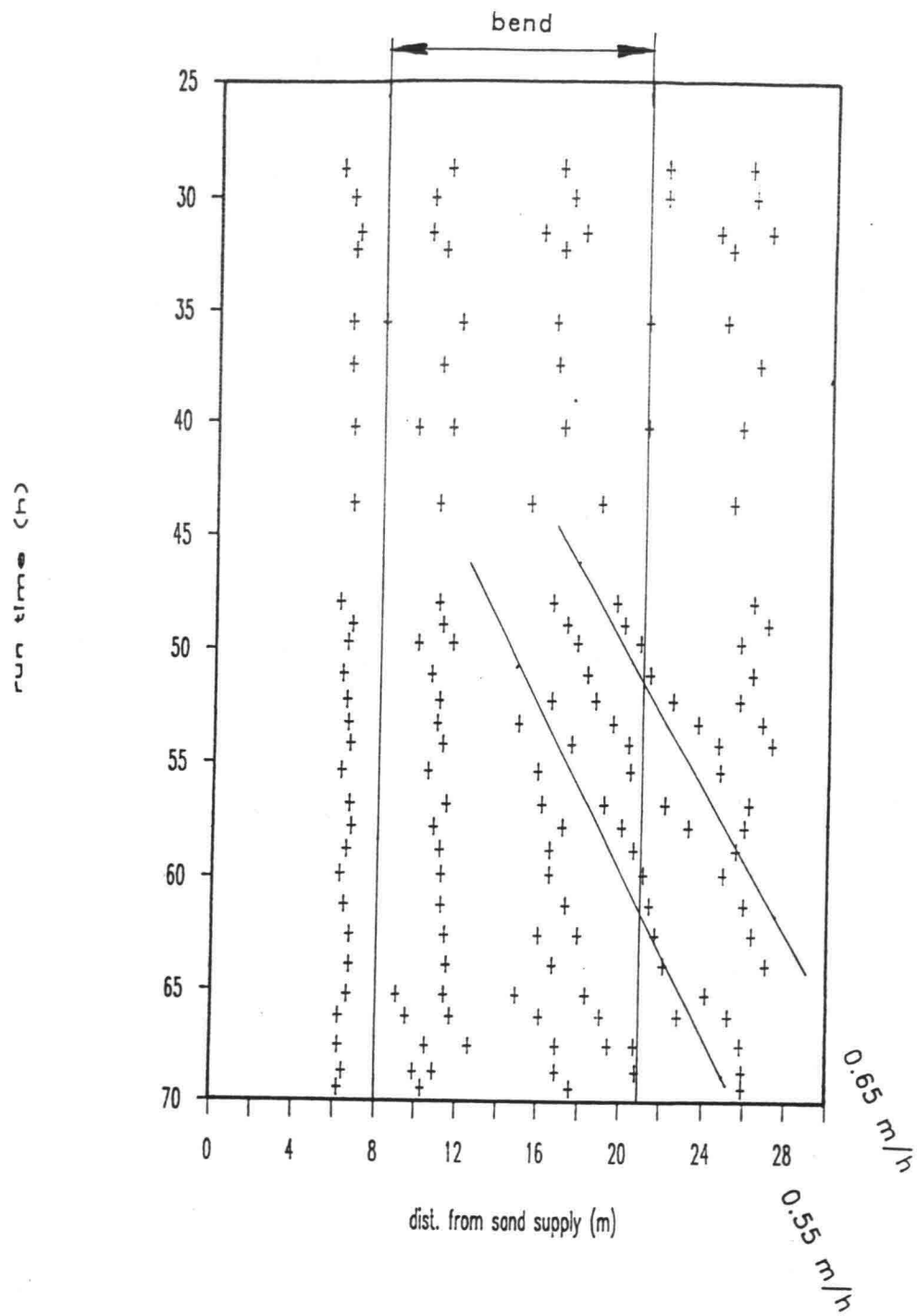
location in cross- direction	Mean water depth	Distance beneath water surface	Concen- tration					
[y/W]	[mm]	[mm]	[g/l]					
1/2	33	5	0.277	0.374	0.513	0.606		
		8	0.448					
		10	0.642	0.686	0.562	0.646	0.558	0.619
			0.588	0.583				
		13	0.954					
		15	0.718	1.243	0.921	0.652	1.395	0.616
			0.669	0.538				
		20	1.259	1.284	1.764	0.871	1.194	
25	1.236	1.307	1.487	1.978	1.884			

Appendix C: Free bars.

Free bars are observed during the pilot experiment, section 3.1, and the bend measurement, section 3.2. The positions of the bars are tracked by visual observation at side walls of the channel.

The results of the pilot experiment in which the flow in the entrance of the straight channel was obstructed are given in fig. C1. The positions of the top (H) and the trough (L) of the bars at the left and the right side walls are given. In the straight channel steady bars are observed, wave length 6.5 m. These are forced by the obstruction. In the bend non-stationary downstream migrating bars are observed, wave length: 3...4 m, celerity: 0.55...0.65 m/h. These are free bars.

The bar observations during the bend measurement are given in fig. C2. The free bar wave length is: 3.2 m, celerity 0.60 m/h.

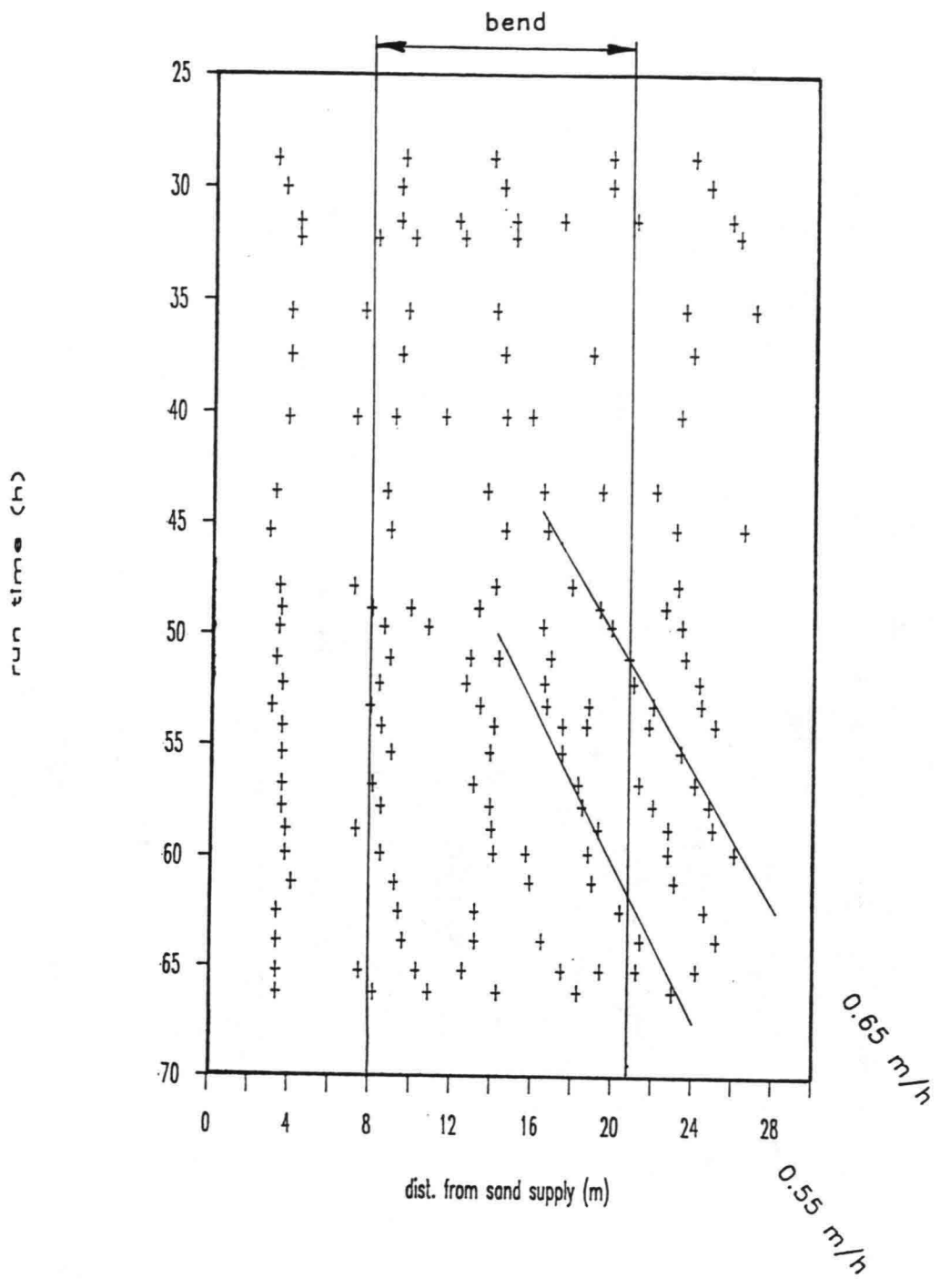


BARS DURING PILOT EXPERIMENT

POSITION FREE BARS CREST, INNERSIDE BEND

DELFT UNIVERSITY OF TECHNOLOGY

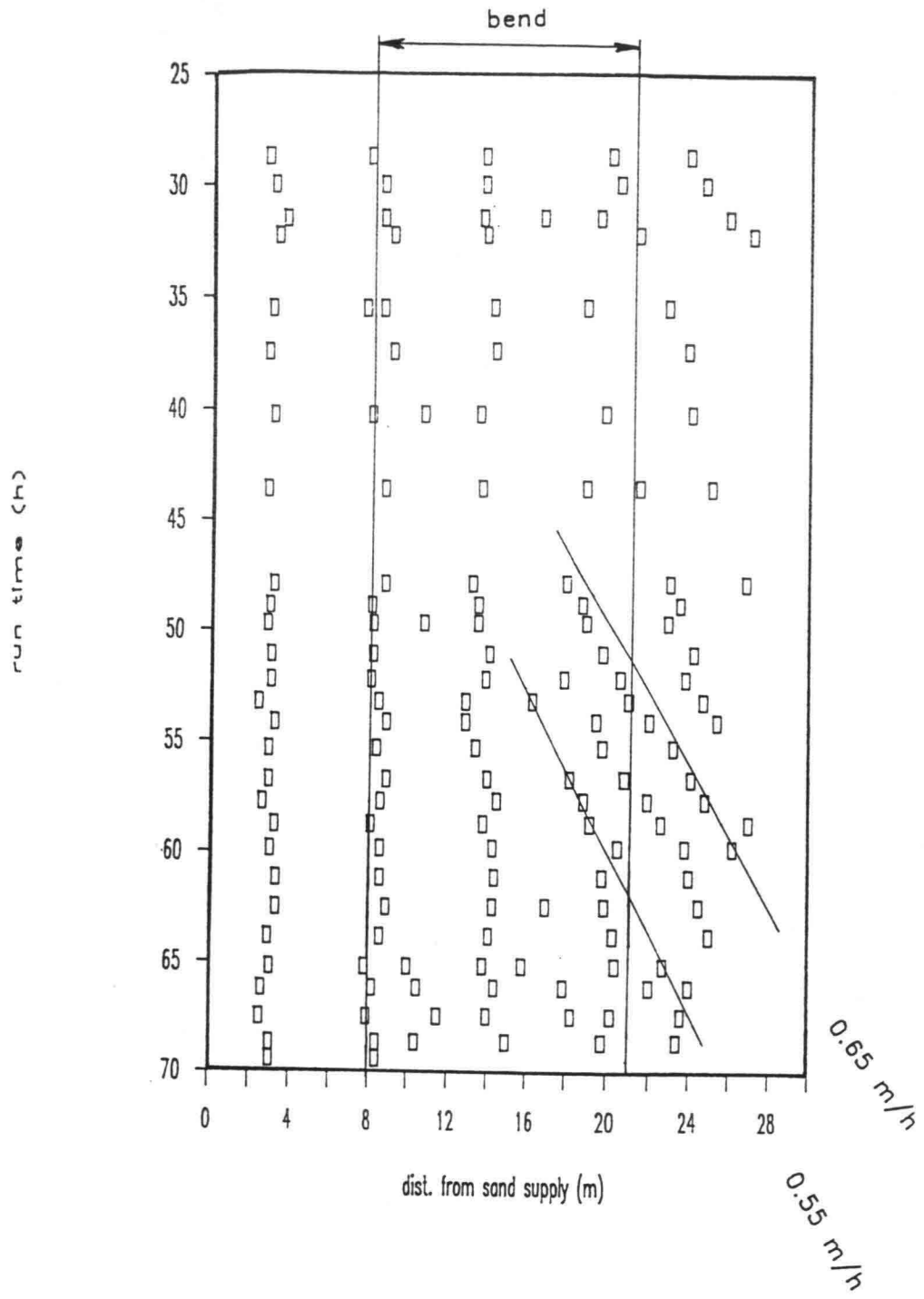
FIG. C1.1



BARS DURING PILOT EXPERIMENT
 POSITION BAR CREST, OUTER SIDE BEND

DELFT UNIVERSITY OF TECHNOLOGY

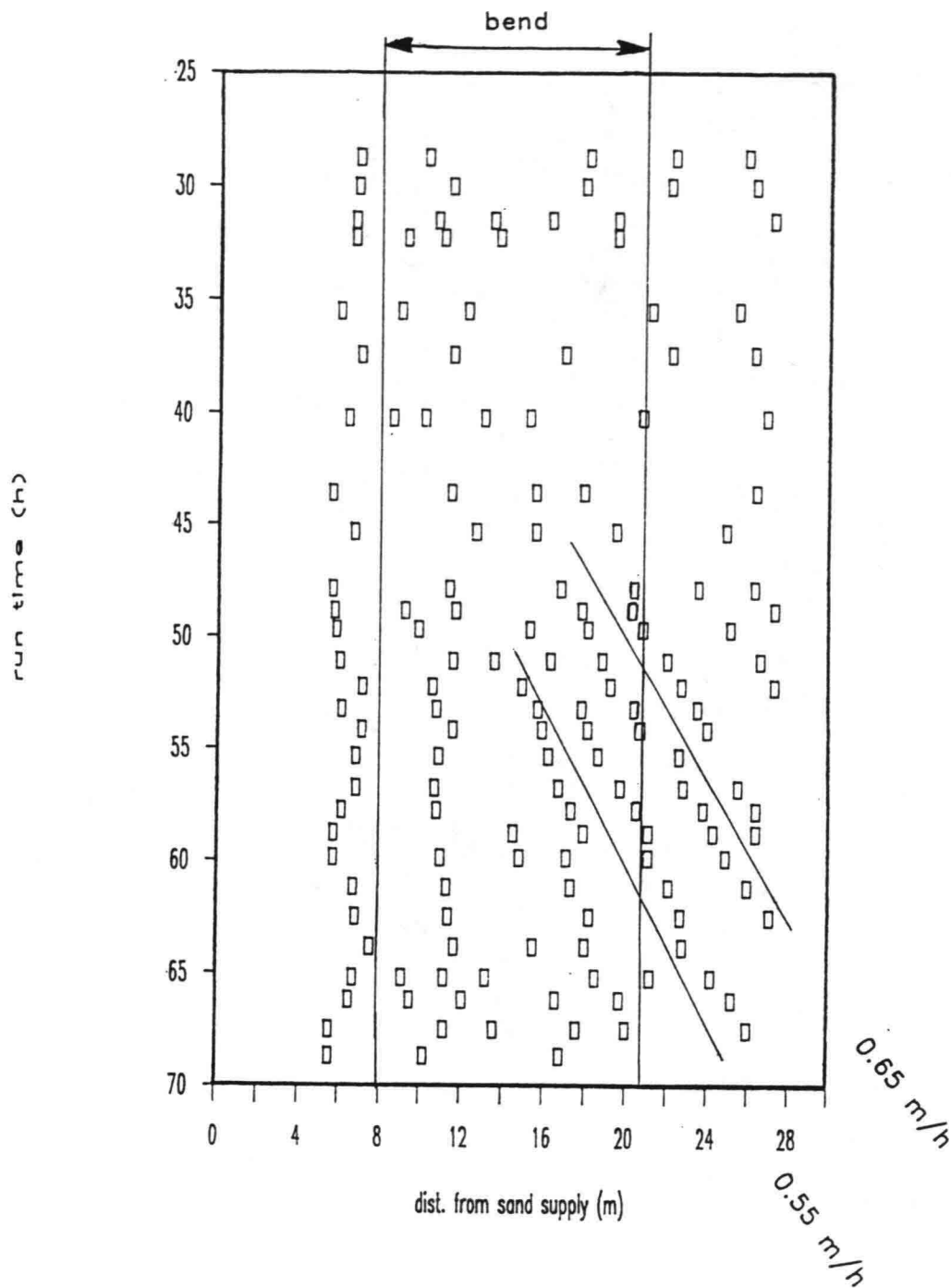
FIG. C1.2



BARS DURING PILOT EXPERIMENT
 POSITION BAR TROUGH, INNER SIDE BEND

DELFT UNIVERSITY OF TECHNOLOGY

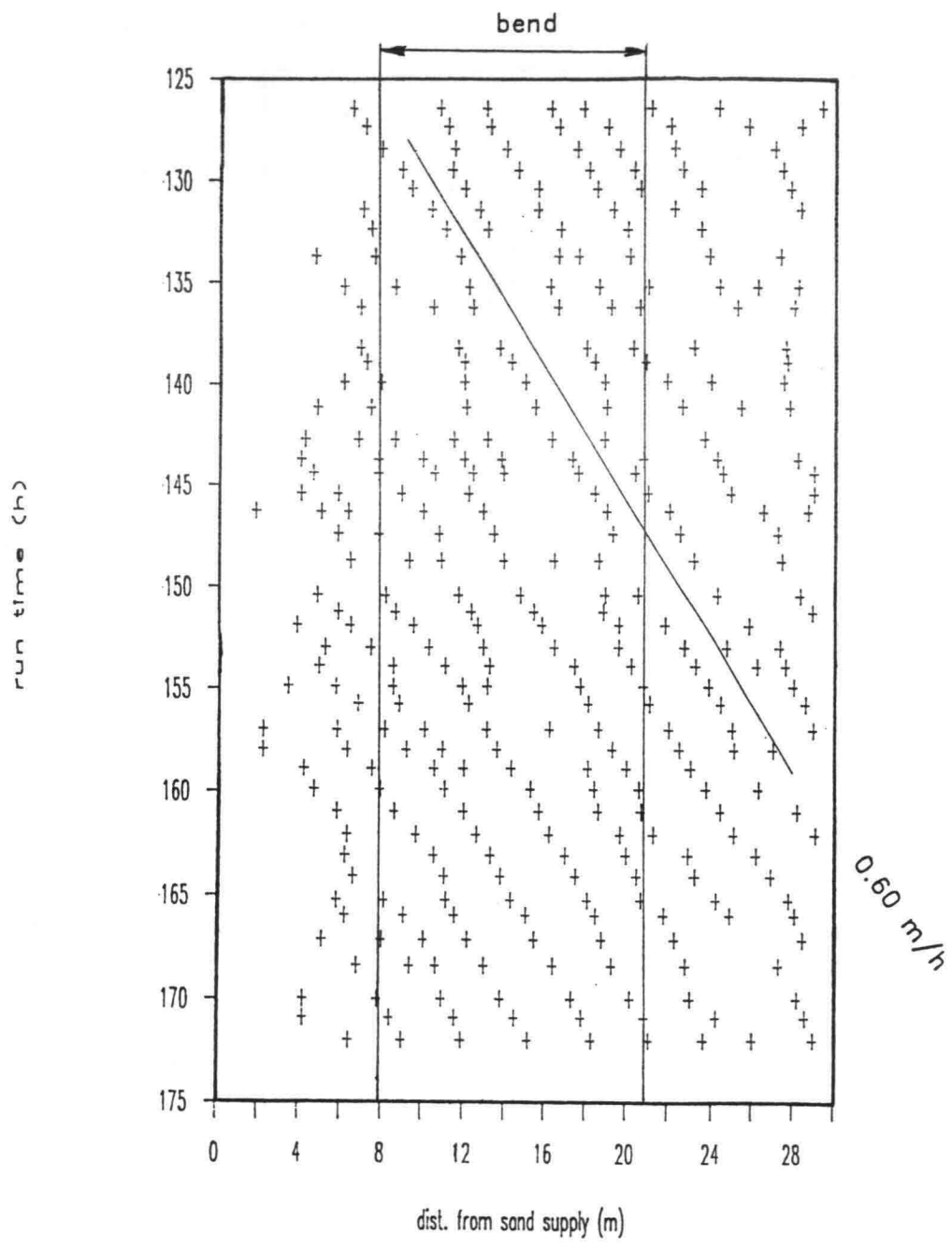
FIG. C1.3



BARS DURING PILOT EXPERIMENT
 POSITION BAR TROUGH, OUTER SIDE BEND

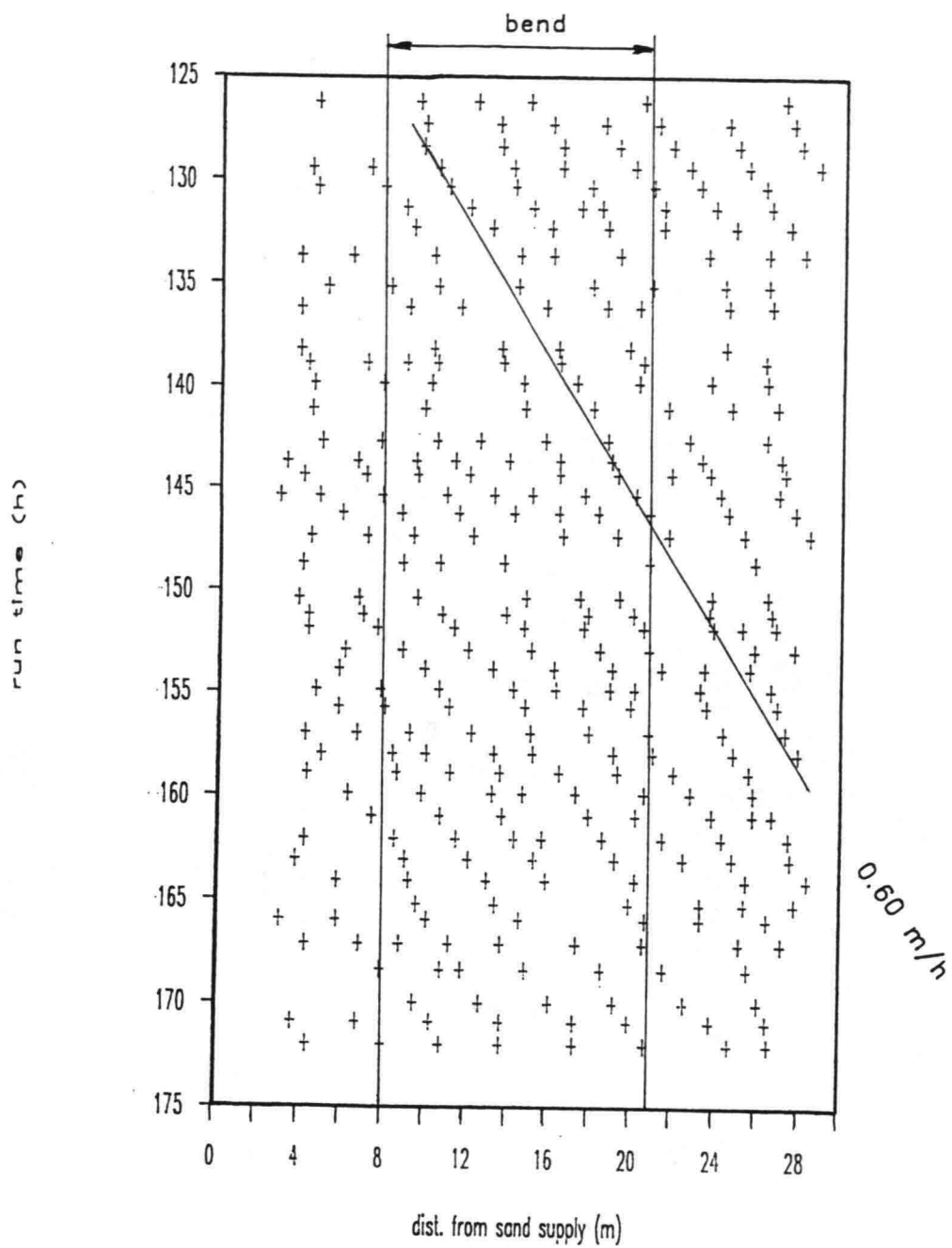
DELFT UNIVERSITY OF TECHNOLOGY

FIG. C1.4



BARS DURING BEND MEASUREMENT
 POSITION BAR CREST, INNER SIDE BEND

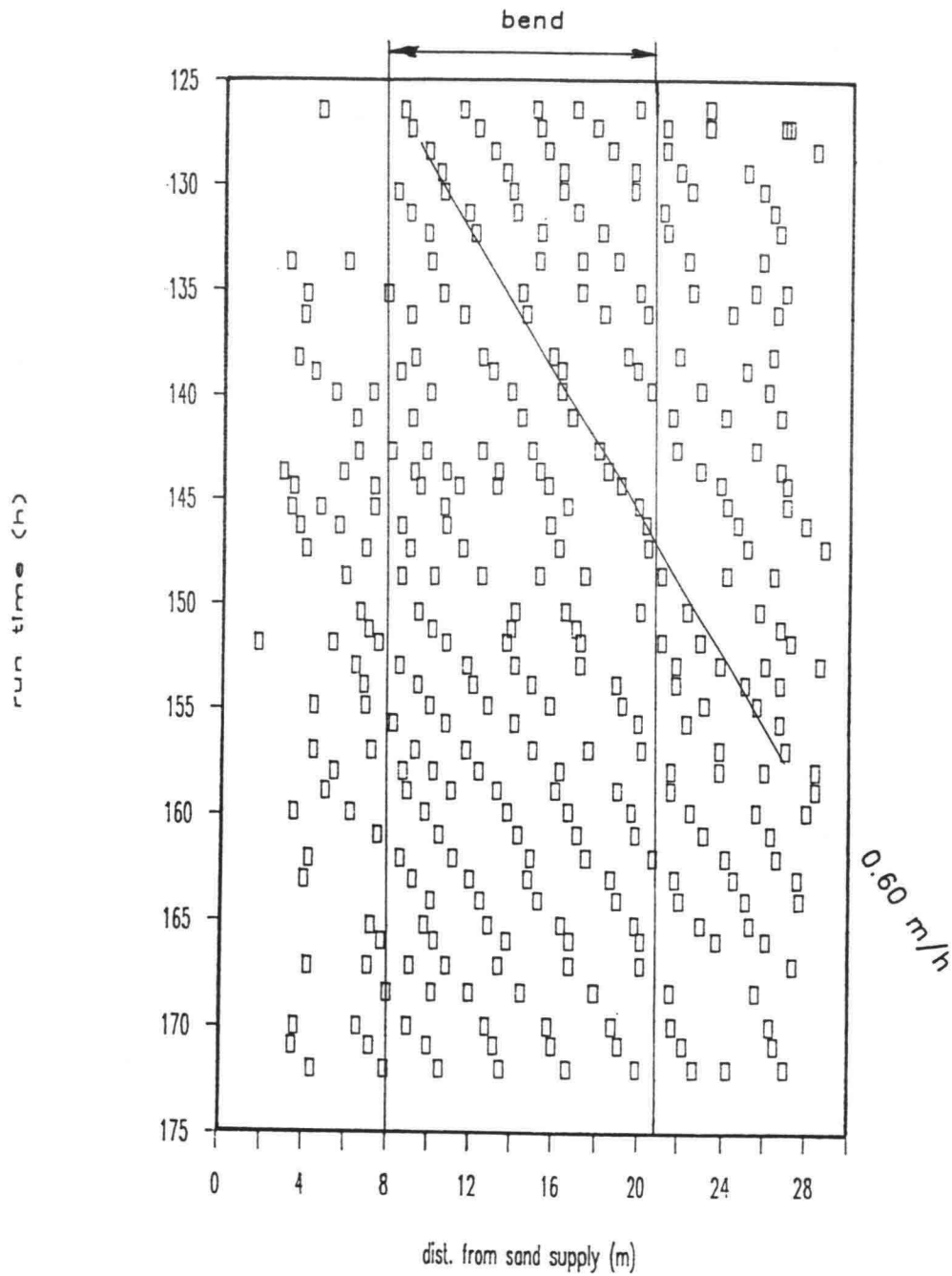
FIG. C2.1



BARS DURING BEND MEASUREMENT
 POSITION BAR CREST, OUTER SIDE BEND

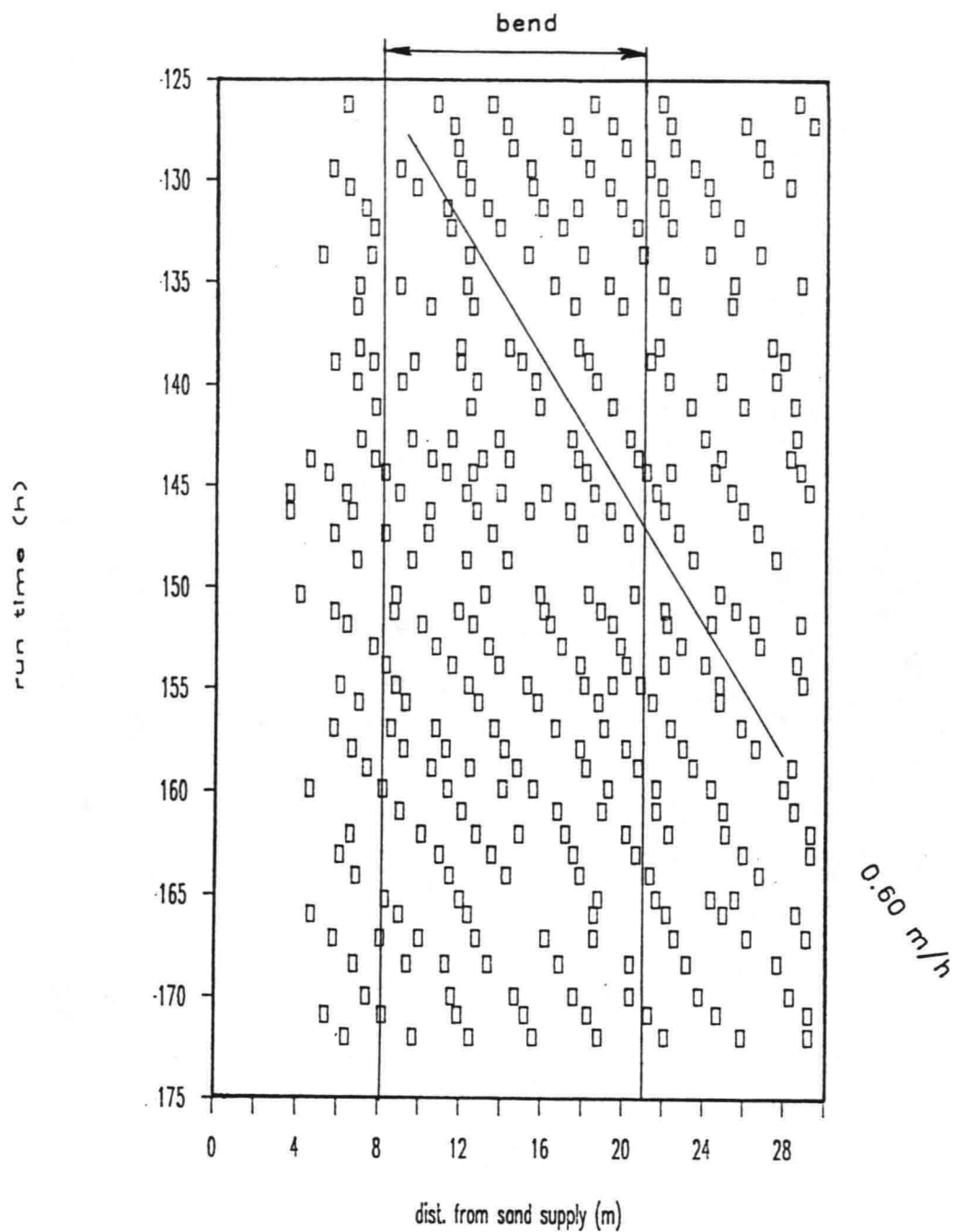
DELFT UNIVERSITY OF TECHNOLOGY

FIG. C2.2



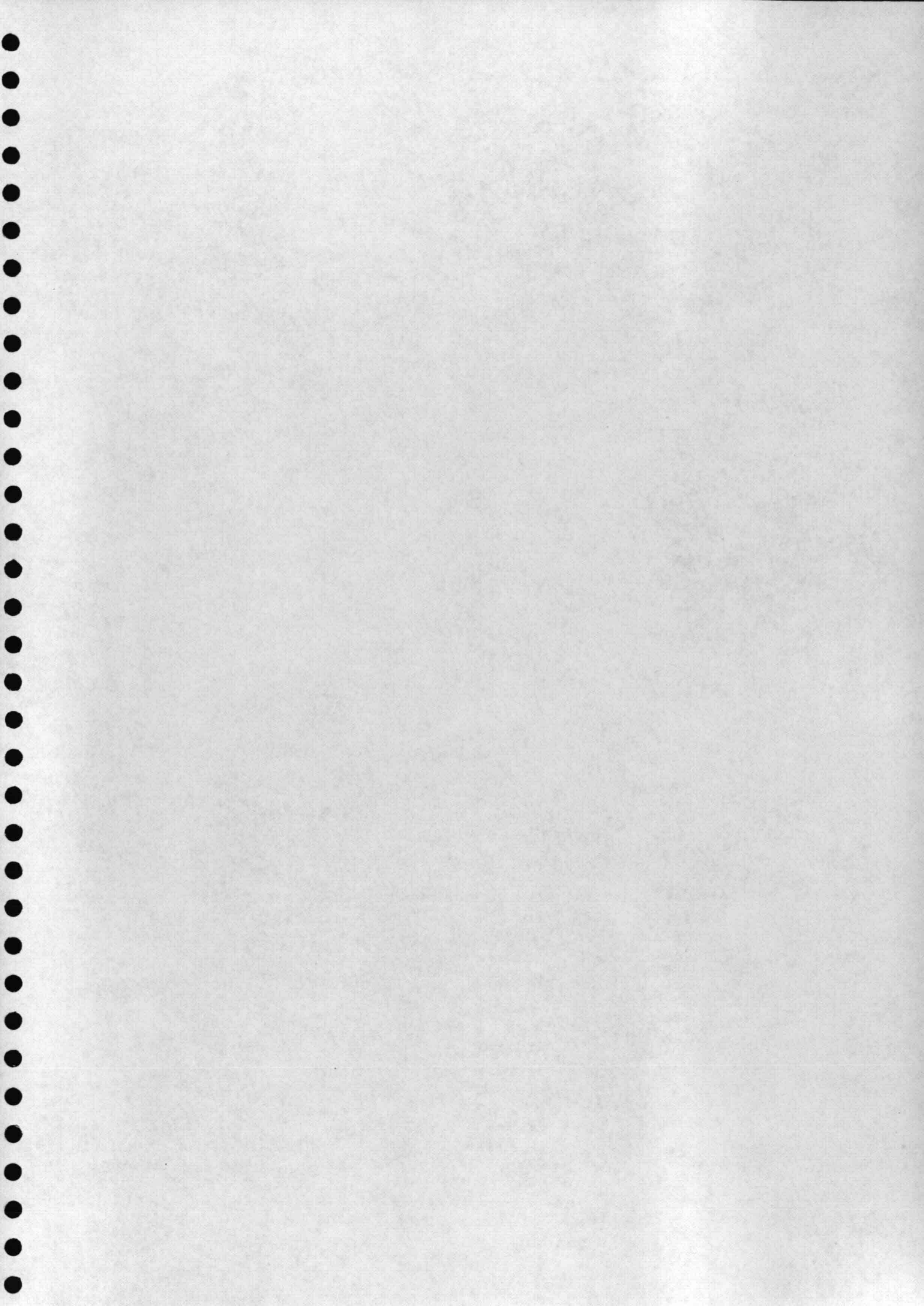
BARS DURING BEND MEASUREMENT
 POSITION BAR TROUGH, INNER SIDE BEND

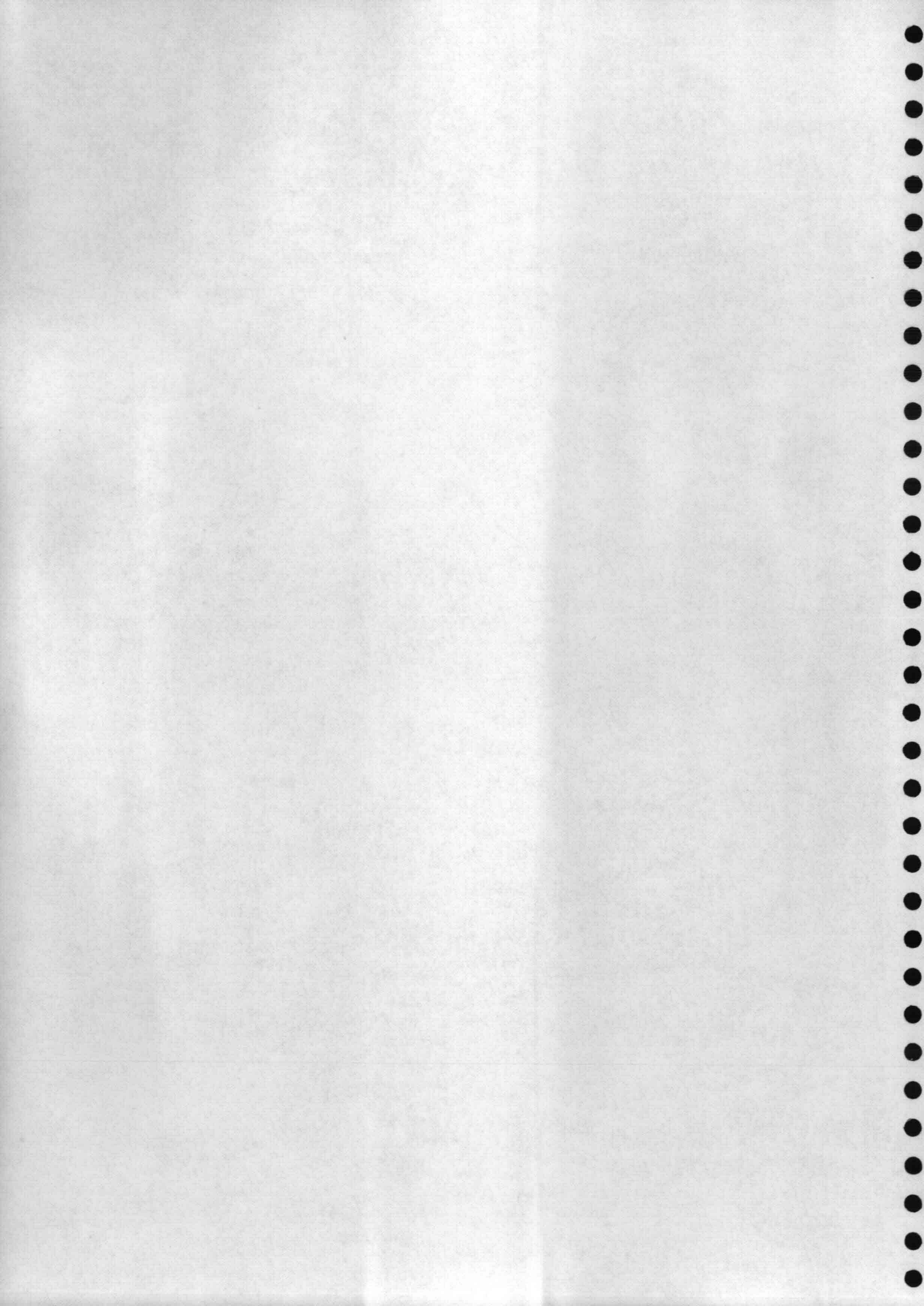
FIG. C2.3

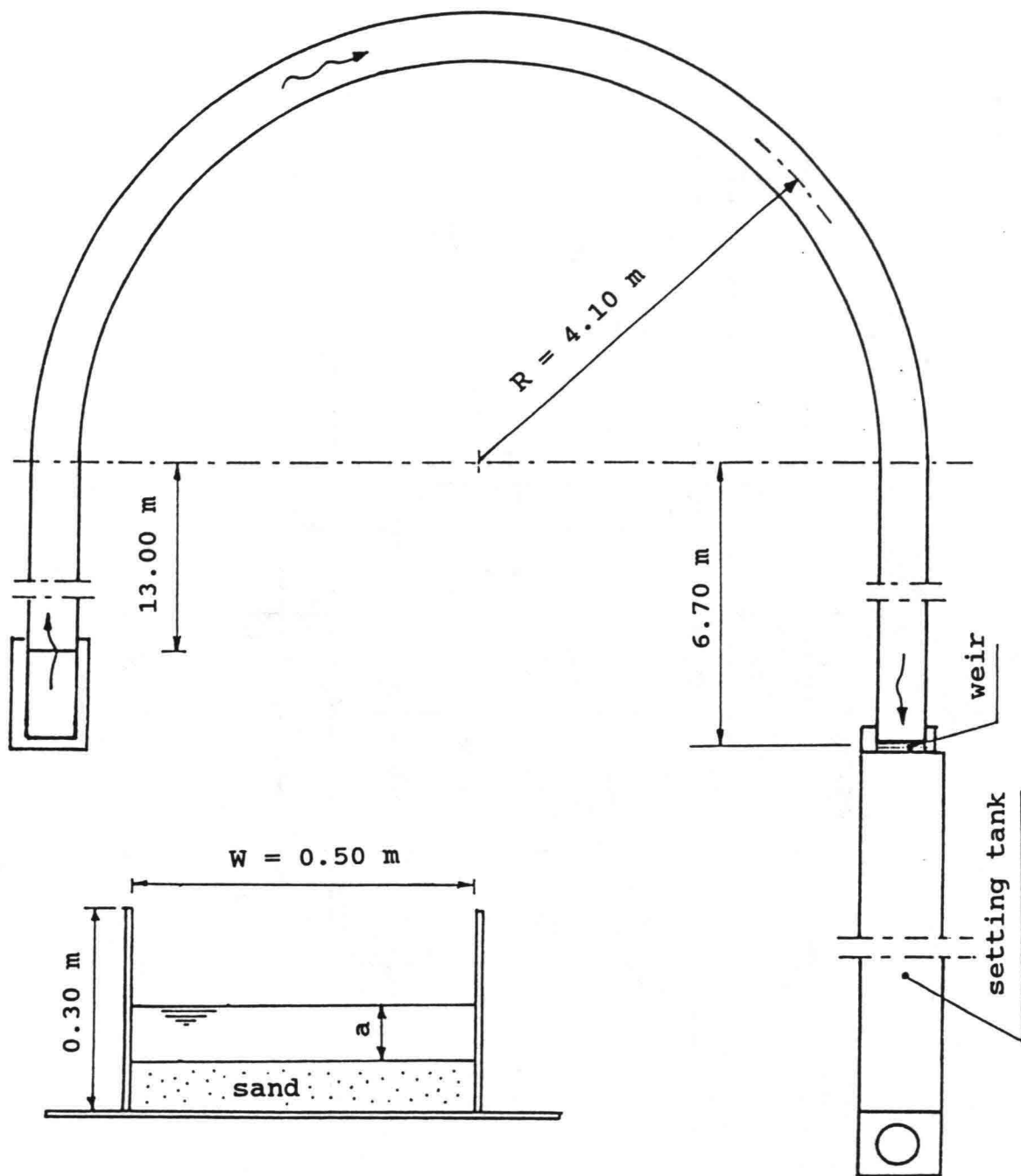


BARS DURING BEND MEASUREMENT
 POSITION BAR TROUGH, OUTER SIDE BEND

FIG. C2.4

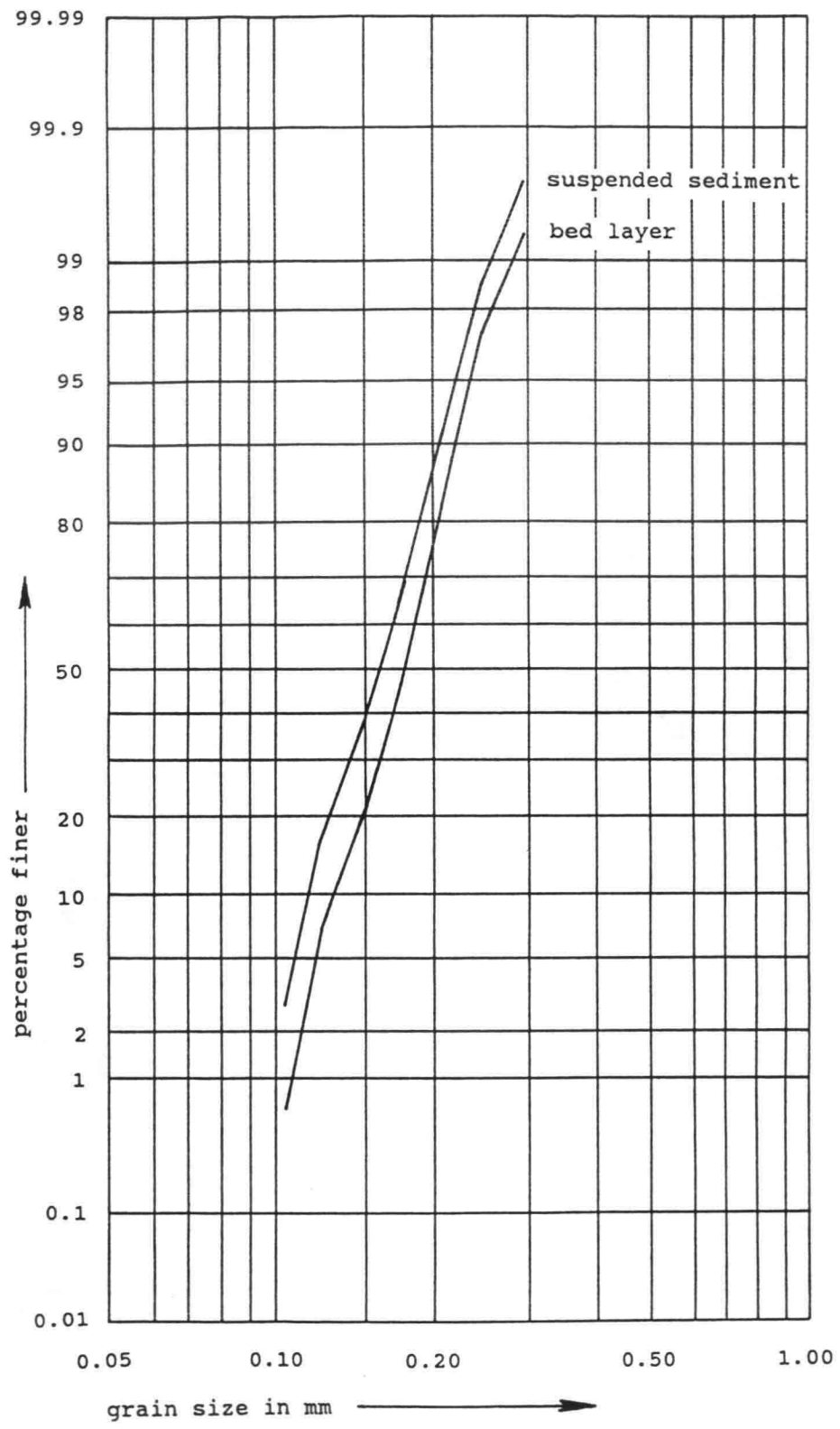






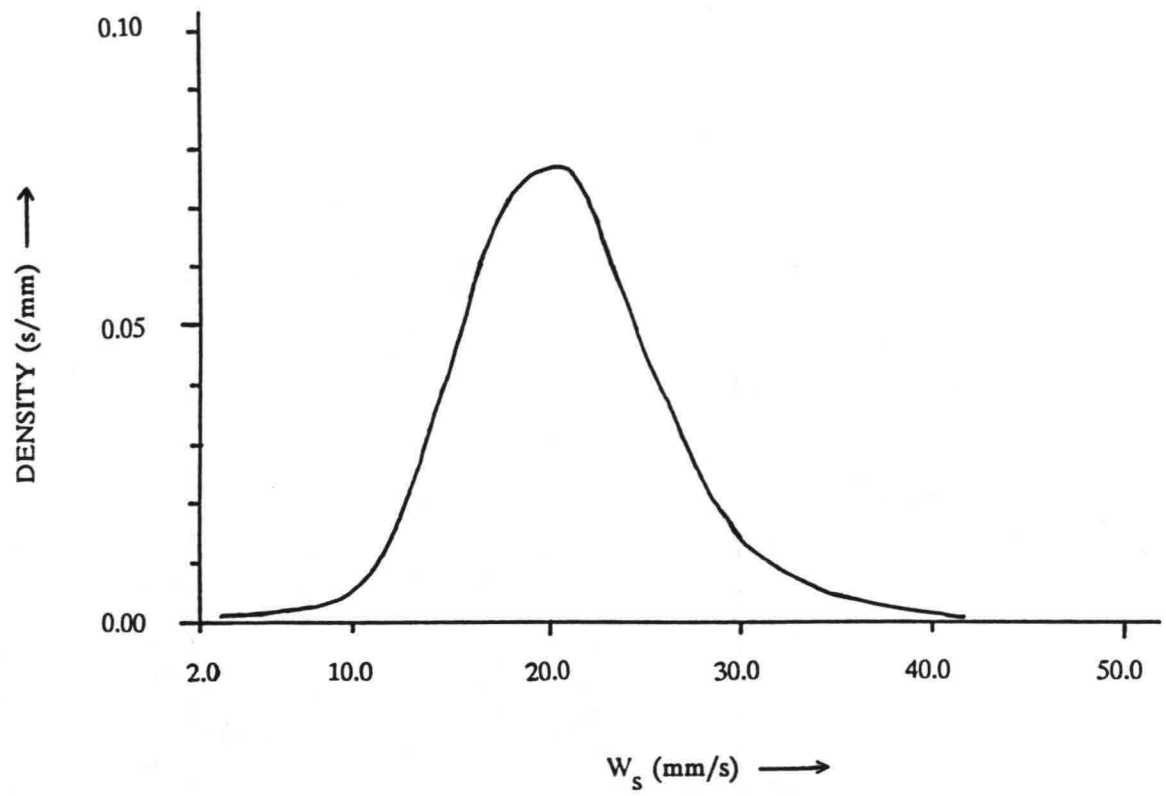
LAYOUT, LFM CURVED FLUME

FIG. 1



SIEVE CURVES OF SEDIMENT

FIG. 2

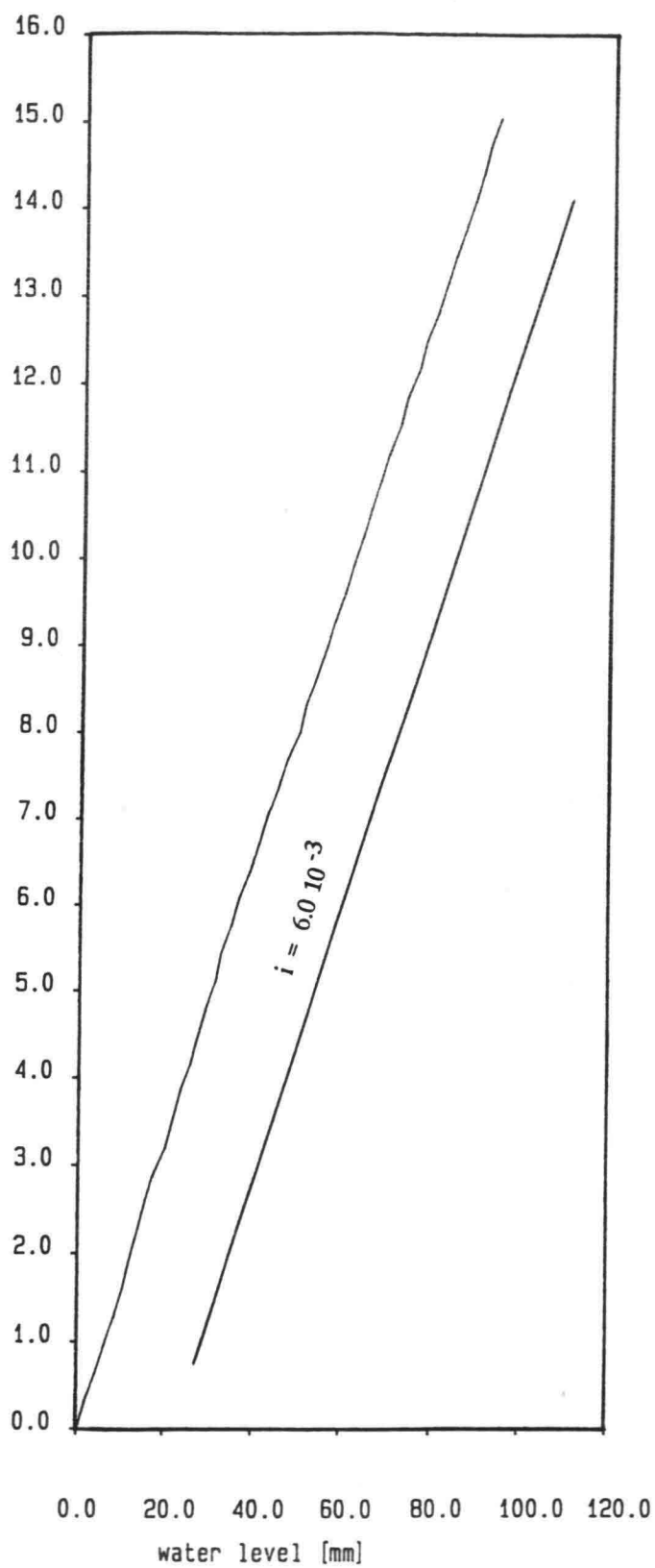


PROBABILITY DENSITY DISTRIBUTION OF FALL VELOCITY

DELFT UNIVERSITY OF TECHNOLOGY

FIG. 3

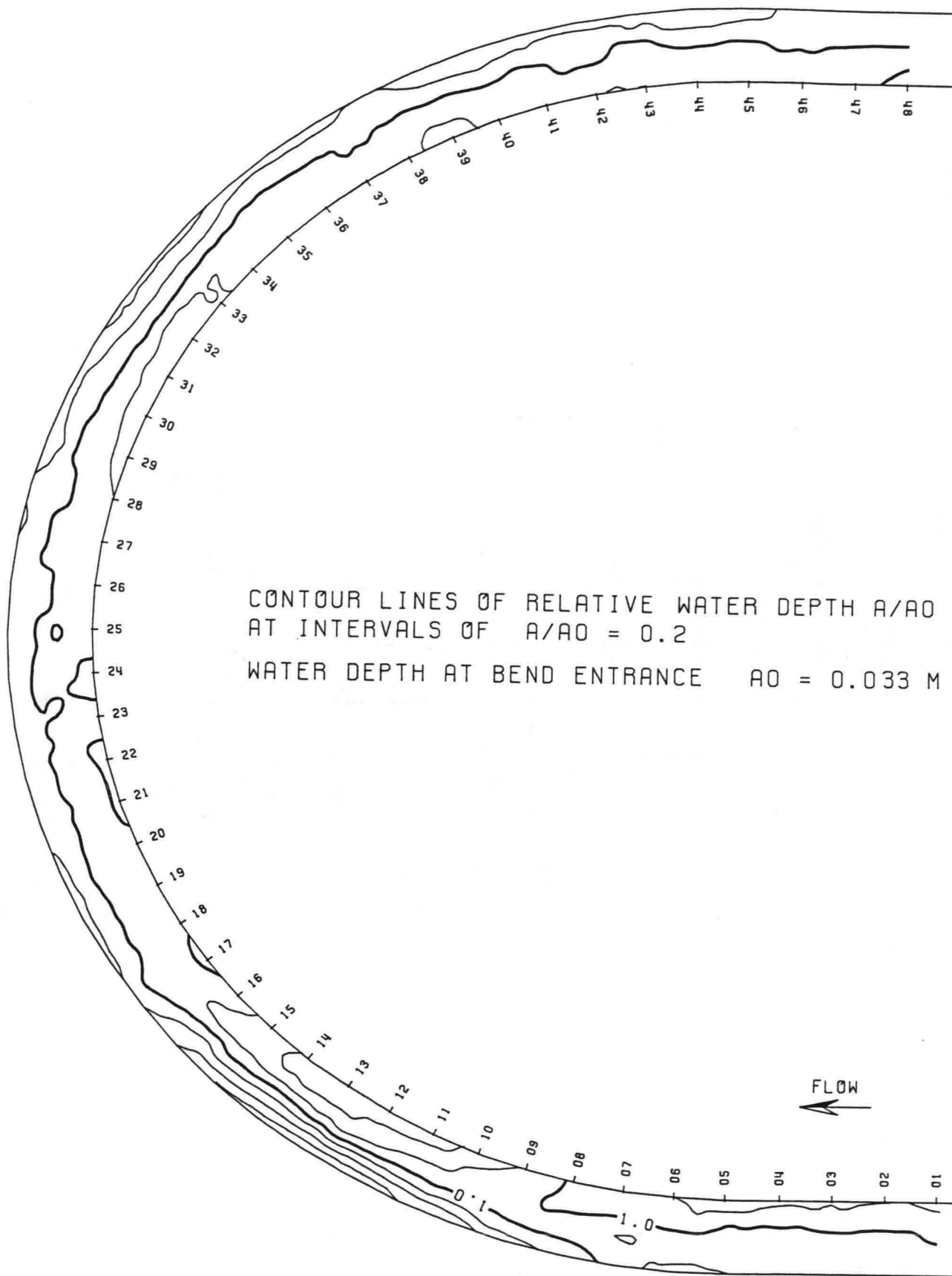
distance [m]



LONGITUDINAL WATER LEVEL SLOPE

FIG. 4

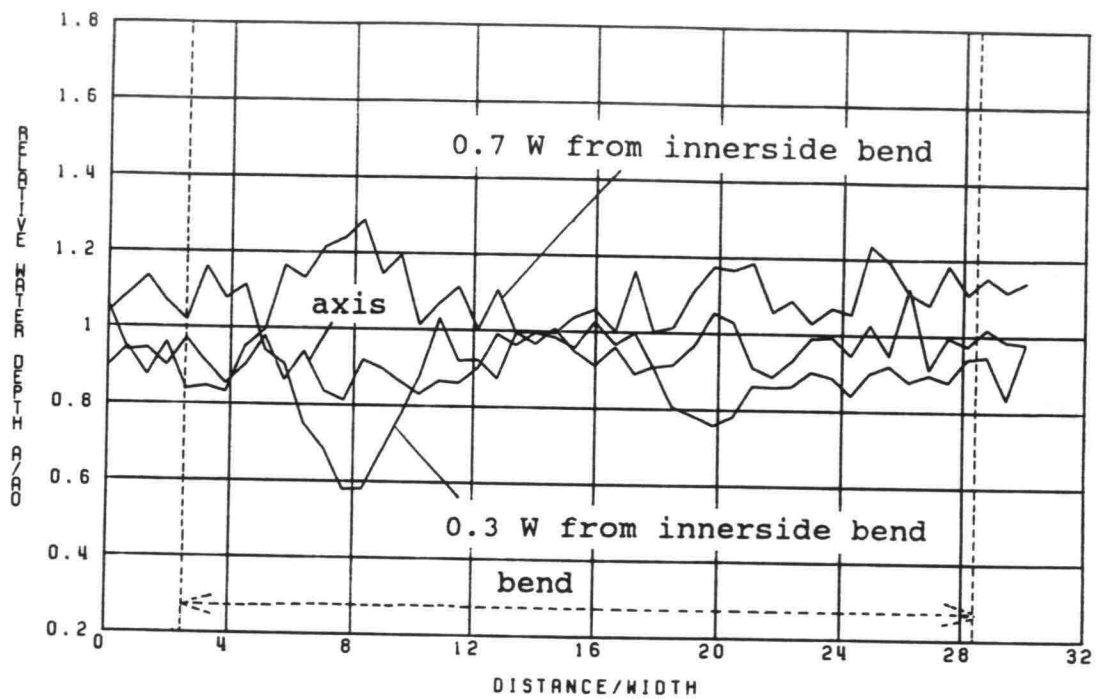
DELFT UNIVERSITY OF TECHNOLOGY



MODEL OF RIVER BEND, SUSPENDED-LOAD EXPERIMENT
 ENSEMBLE MEAN OF 21 LONGITUDINAL TRAVERSES

FIG. 5

DELFT UNIVERSITY OF TECHNOLOGY

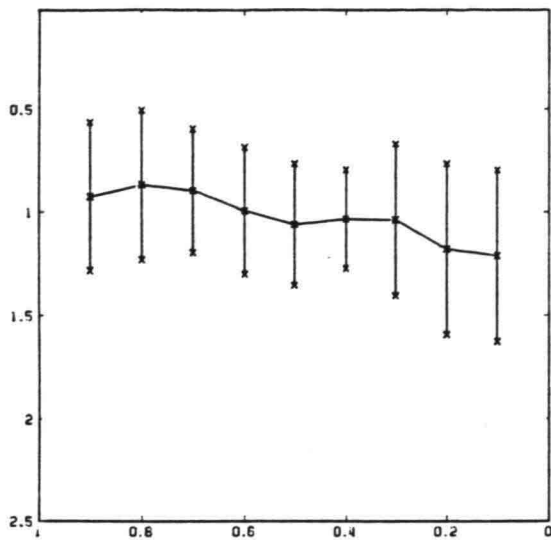


W = 0.5 M AO = 0.033 M

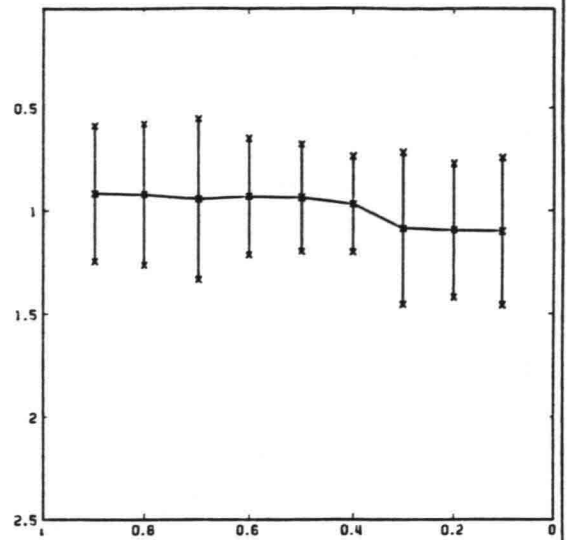
LONGITUDINAL PROFILE OF THE WATER DEPTH

FIG 6

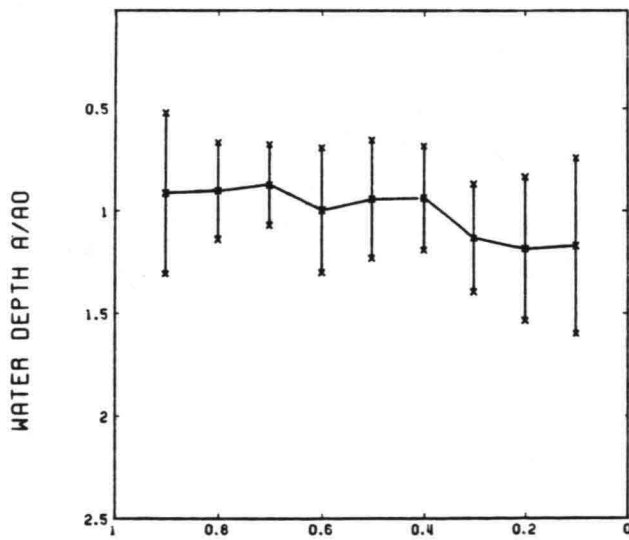
DELFT UNIVERSITY OF TECHNOLOGY



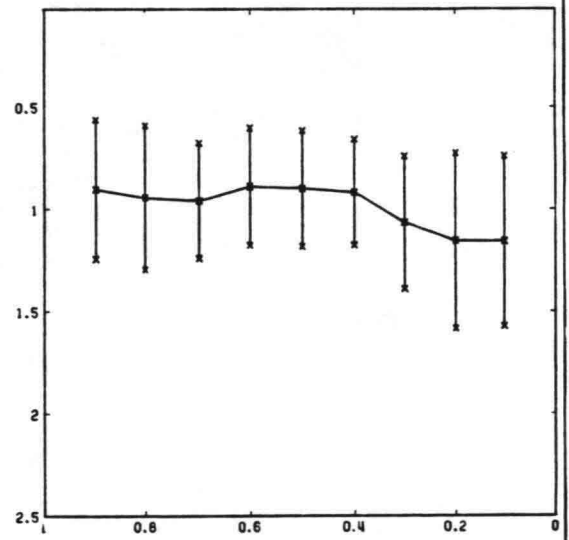
CROSS-SECTION 1



CROSS-SECTION 2



CROSS-SECTION 3



CROSS-SECTION 4

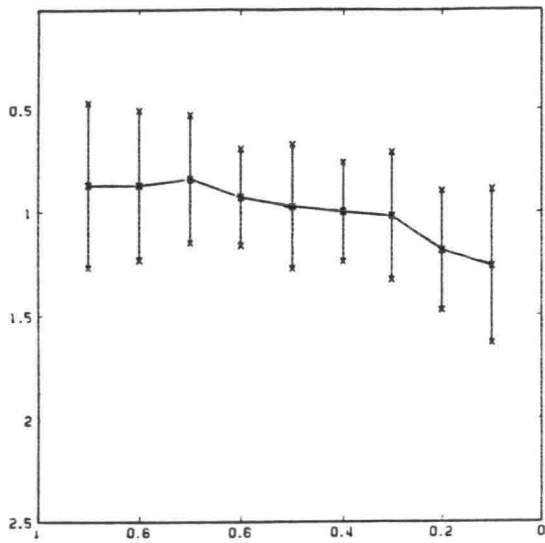
W = 0.5 M RO = 0.033 M

$\pm \sigma$ OF 21 MEASUREMENTS

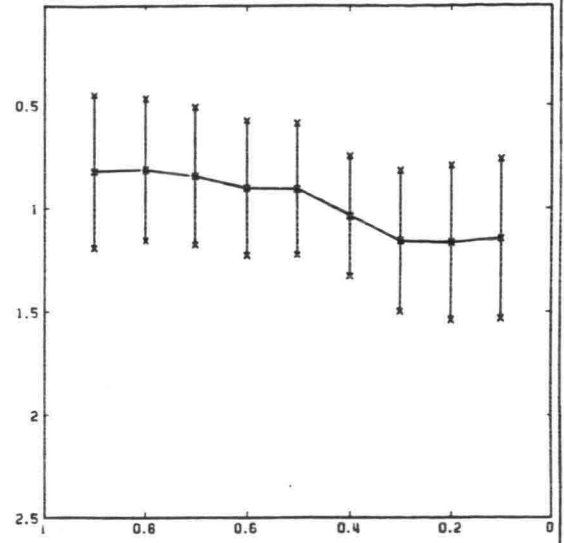
WATER DEPTH IN CROSS-DIRECTION

FIG 7A

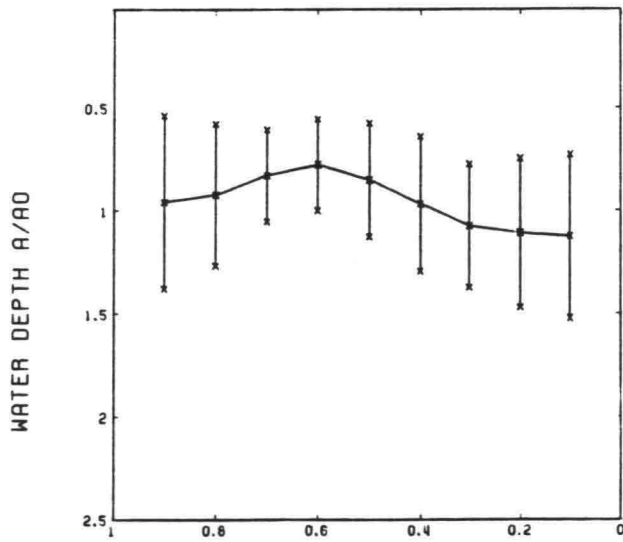
DELFT UNIVERSITY OF TECHNOLOGY



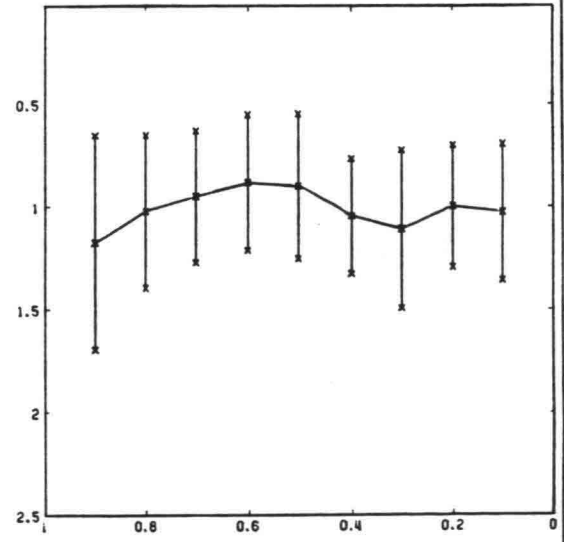
CROSS-SECTION 5



CROSS-SECTION 6



CROSS-SECTION 7



CROSS-SECTION 8

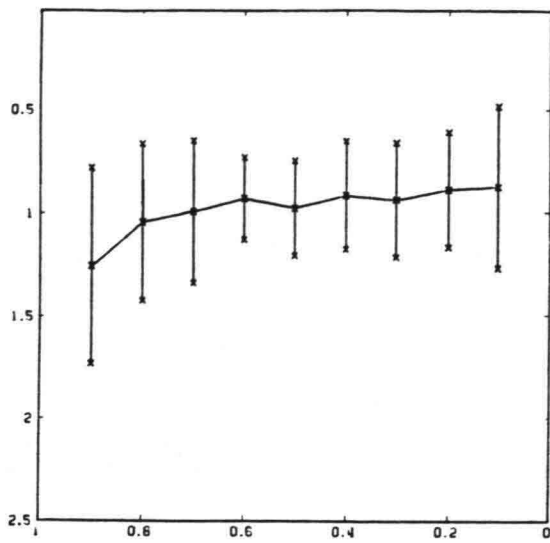
W = 0.5 M AO = 0.033 M

$\pm \sigma$ OF 21 MEASUREMENTS

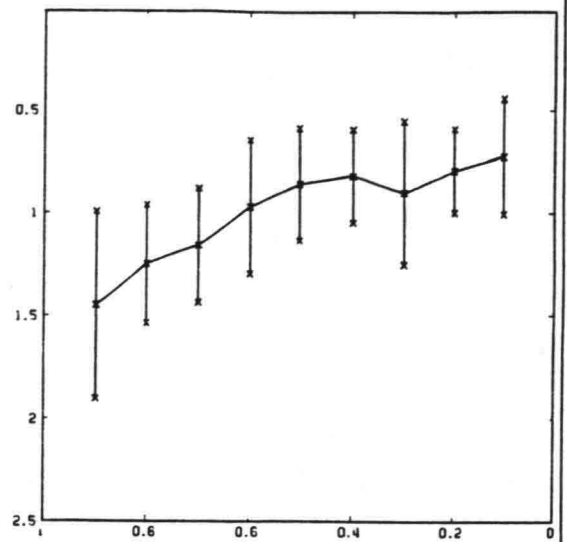
WATER DEPTH IN CROSS-DIRECTION

FIG 7B

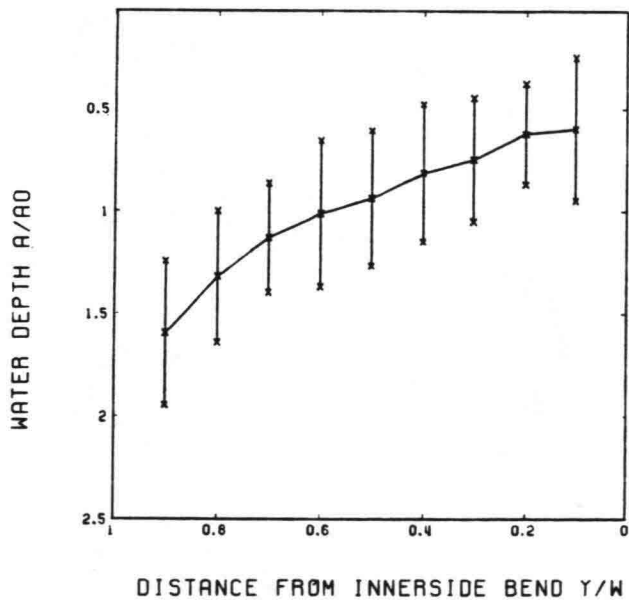
DELFT UNIVERSITY OF TECHNOLOGY



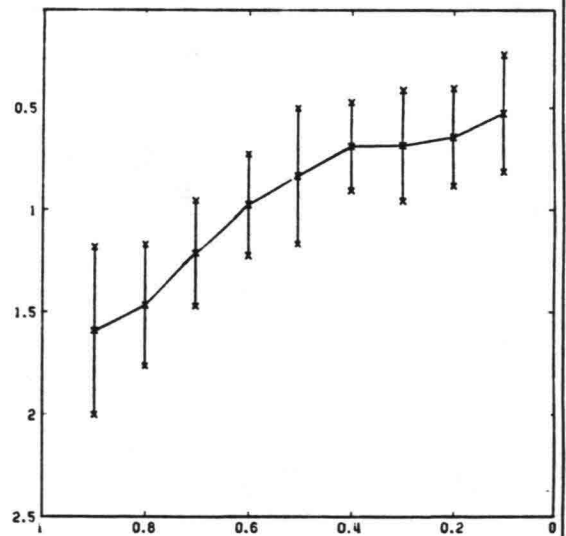
CROSS-SECTION 9



CROSS-SECTION 10



CROSS-SECTION 11



CROSS-SECTION 12

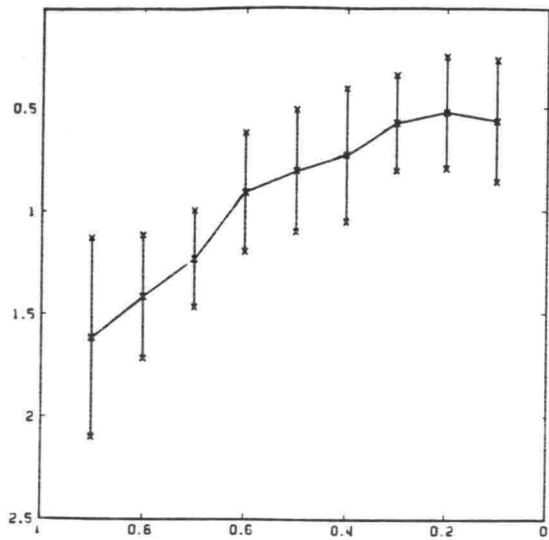
W = 0.5 M RO = 0.033 M

$\bar{x} \pm \sigma$ OF 21 MEASUREMENTS

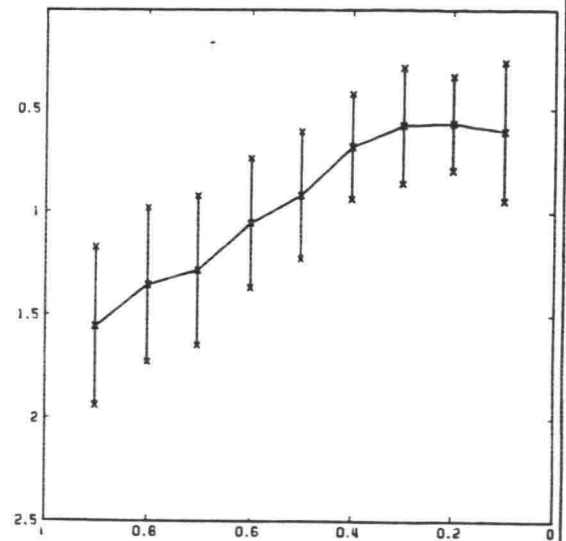
WATER DEPTH IN CROSS-DIRECTION

FIG 7C

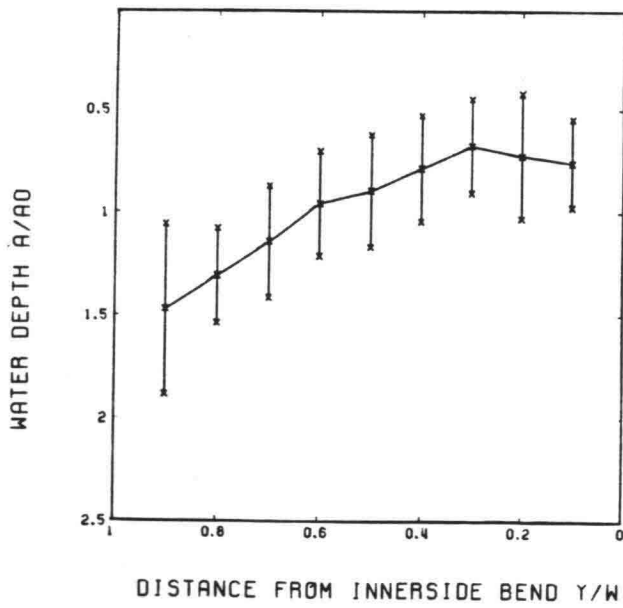
DELFT UNIVERSITY OF TECHNOLOGY



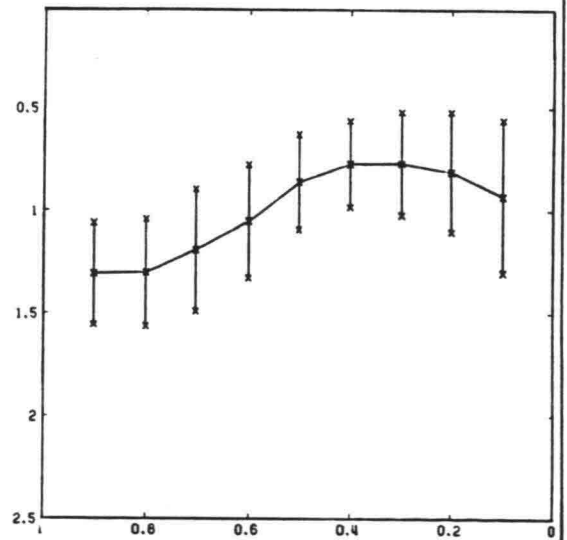
CROSS-SECTION 13



CROSS-SECTION 14



CROSS-SECTION 15



CROSS-SECTION 16

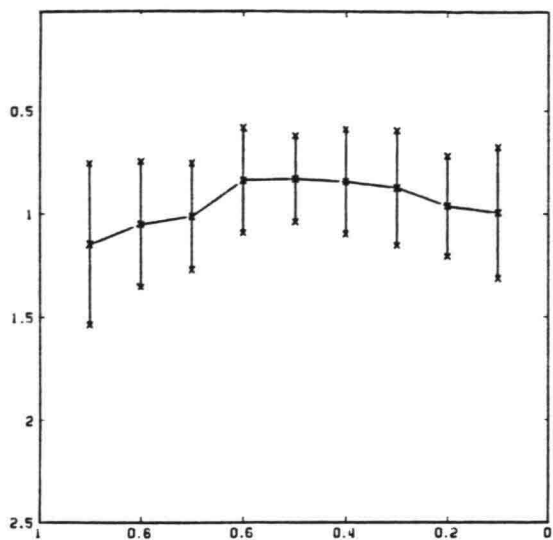
W = 0.5 M A0 = 0.033 M

$\pm \sigma$ OF 21 MEASUREMENTS

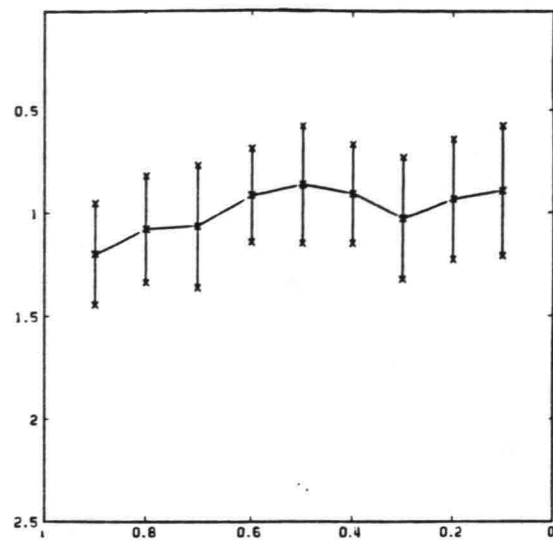
WATER DEPTH IN CROSS-DIRECTION

FIG 7D

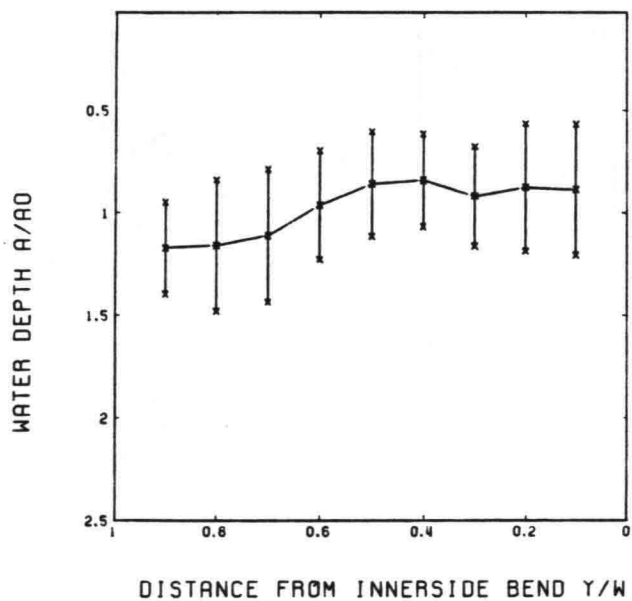
DELFT UNIVERSITY OF TECHNOLOGY



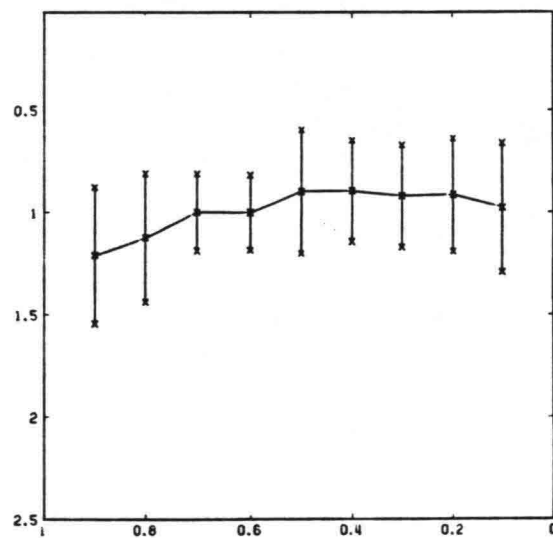
CROSS-SECTION 17



CROSS-SECTION 18



CROSS-SECTION 19



CROSS-SECTION 20

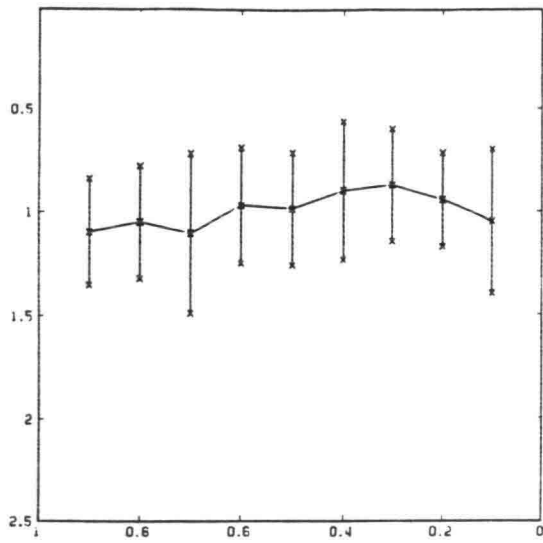
W = 0.5 M A0 = 0.033 M

$\pm \sigma$ OF 21 MEASUREMENTS

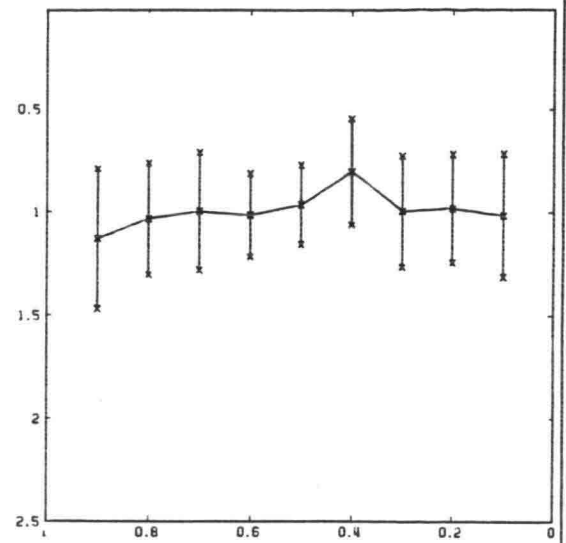
WATER DEPTH IN CROSS-DIRECTION

FIG 7E

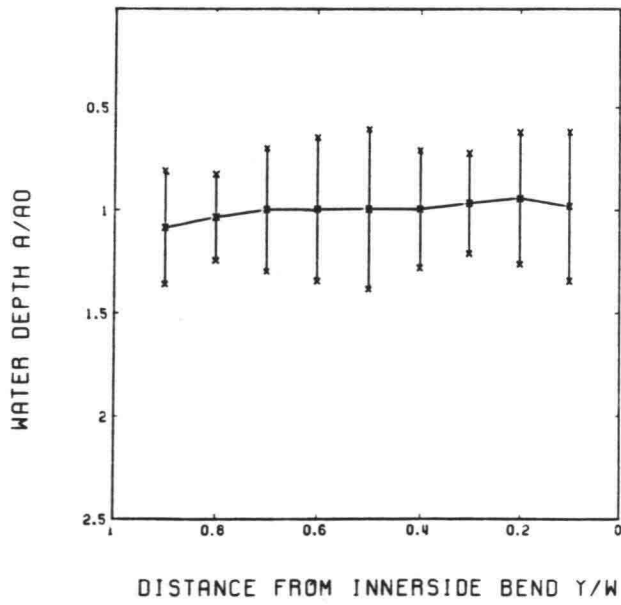
DELFT UNIVERSITY OF TECHNOLOGY



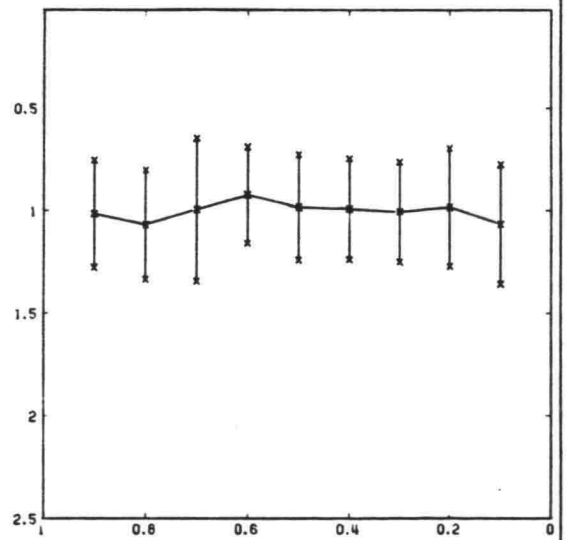
CROSS-SECTION 21



CROSS-SECTION 22



CROSS-SECTION 23



CROSS-SECTION 24

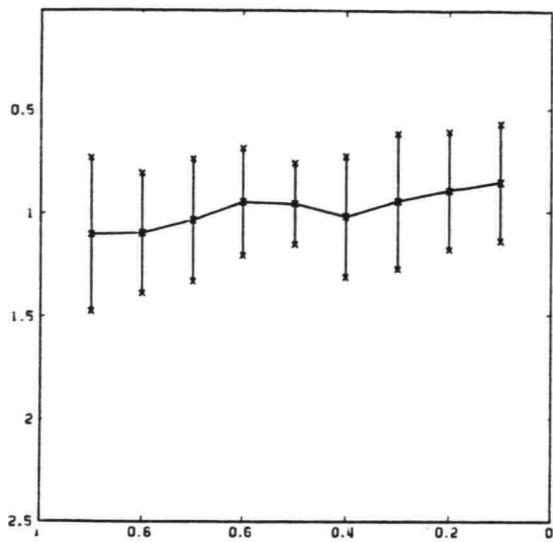
W = 0.5 M A0 = 0.033 M

$\pm \sigma$ OF 21 MEASUREMENTS

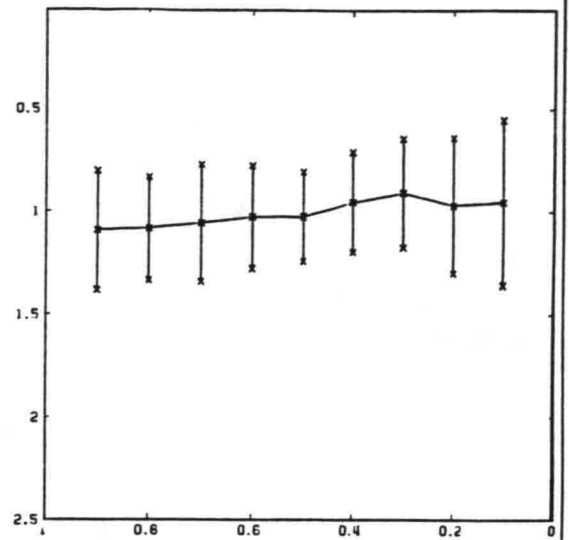
WATER DEPTH IN CROSS-DIRECTION

FIG 7F

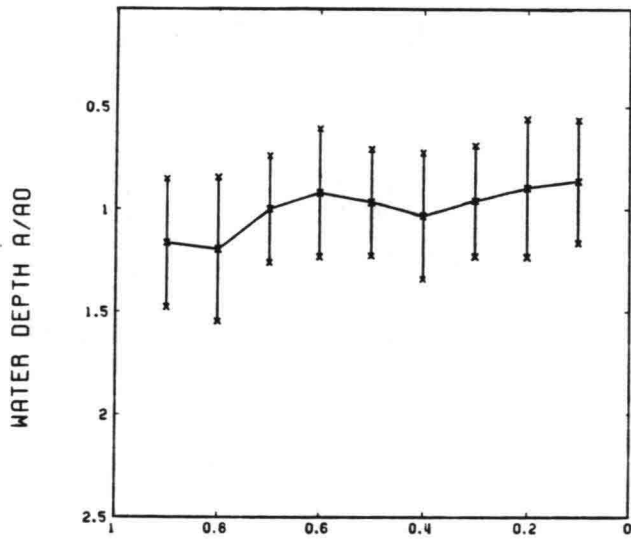
DELFT UNIVERSITY OF TECHNOLOGY



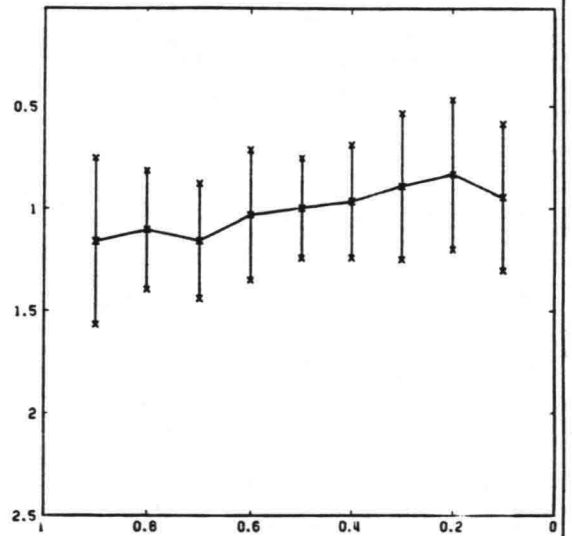
CROSS-SECTION 25



CROSS-SECTION 26



CROSS-SECTION 27



CROSS-SECTION 28

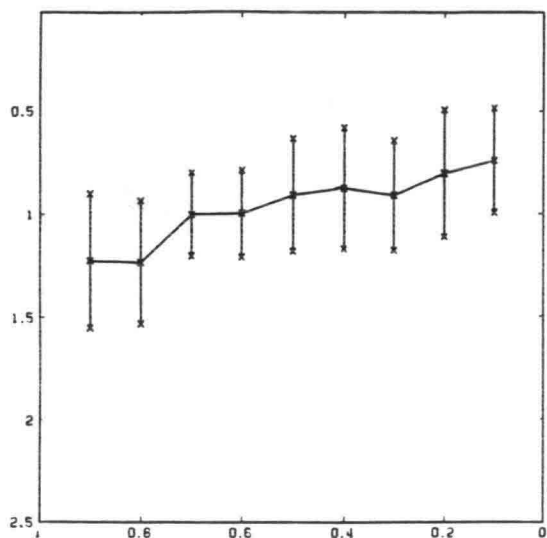
W = 0.5 M AO = 0.033 M

$\pm \sigma$ OF 21 MEASUREMENTS

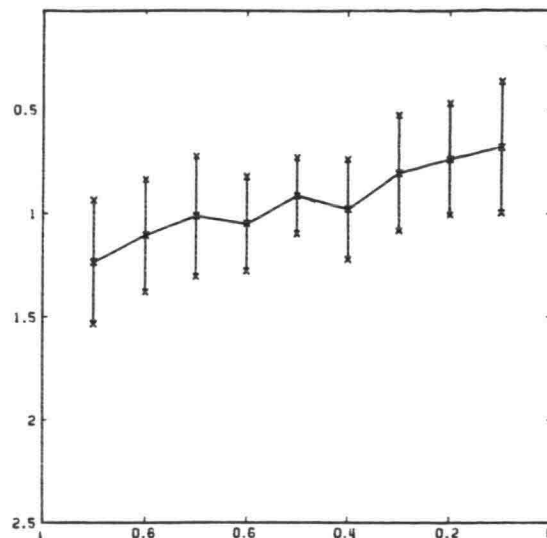
WATER DEPTH IN CROSS-DIRECTION

FIG 7G

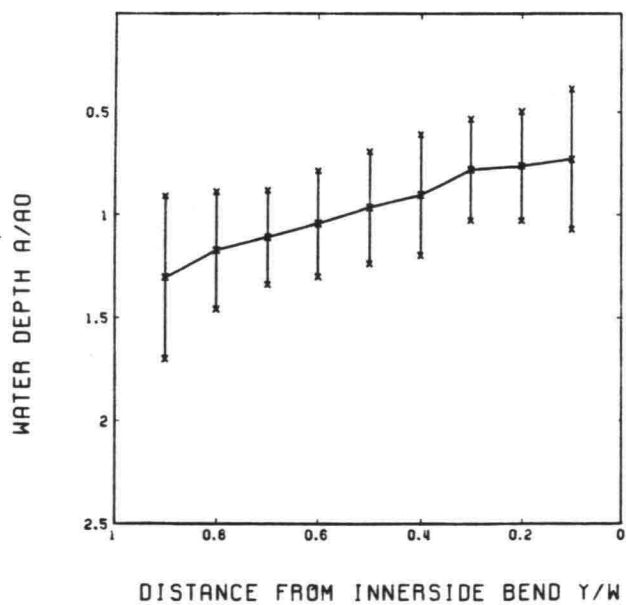
DELFT UNIVERSITY OF TECHNOLOGY



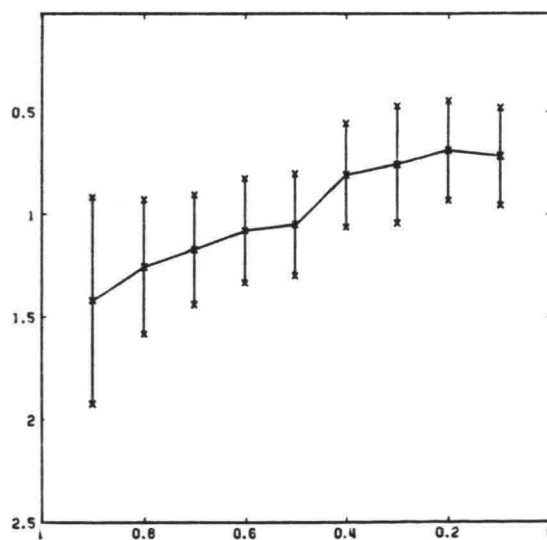
CROSS-SECTION 29



CROSS-SECTION 30



CROSS-SECTION 31



CROSS-SECTION 32

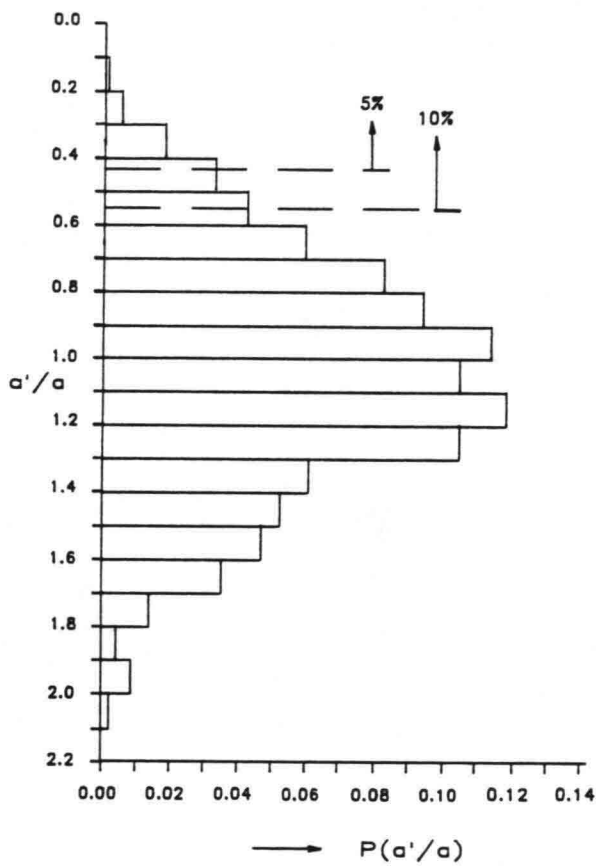
W = 0.5 M A0 = 0.033 M

$\pm \sigma$ OF 21 MEASUREMENTS

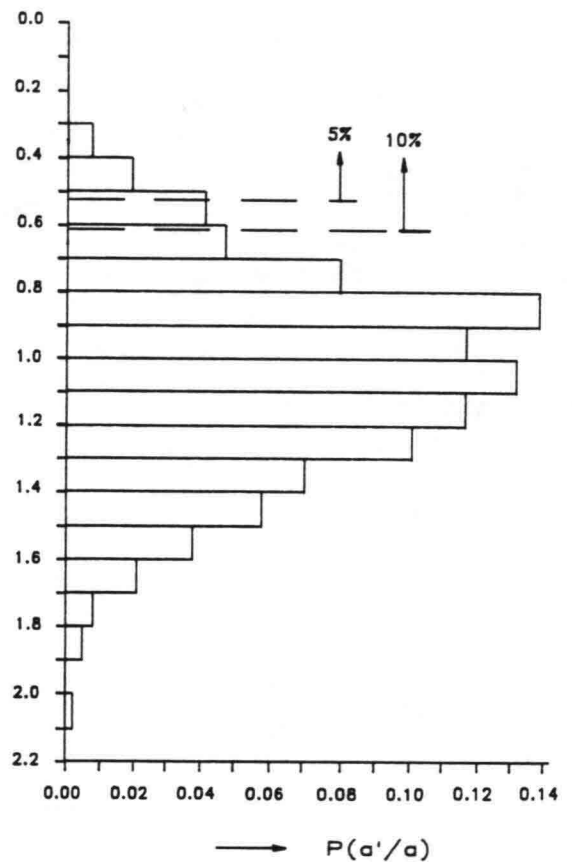
WATER DEPTH IN CROSS-DIRECTION

FIG 7H

DELFT UNIVERSITY OF TECHNOLOGY



CROSS-SECTION 1 TO 5



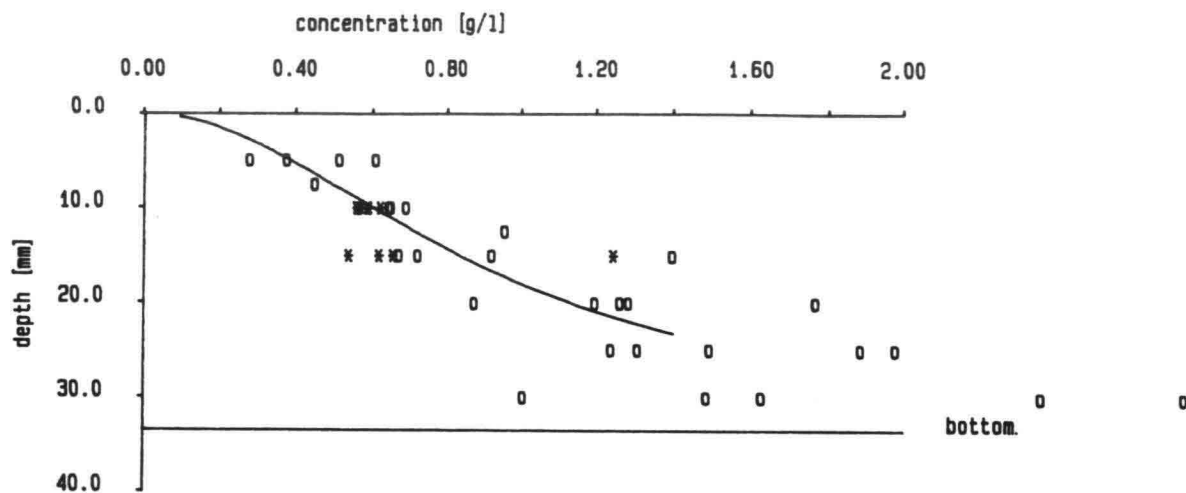
FLUME AXIS

a' local water depth
 a ensemble mean local water depth

PROBABILITY DISTRIBUTION OF BED LEVEL

FIG. 8

DELFT UNIVERSITY OF TECHNOLOGY



CONCENTRATIONS AT CROSS-SECTION 1
 + CURVE FIT BY ROUSE PROFILE

FIG. 9

DELFT UNIVERSITY OF TECHNOLOGY

